BROAD-LINE NMR INVESTIGATION OF THE AMORPHOUS COMPONENT IN POLY(TRANS 1,4 BUTADIENE) AND POLY(4 METHYLPENTENE 1) CRYSTALS WETTED BY CARBON DISULFIDE

BY

KENNETH S-B ENG

A dissertation submitted to the Graduate Faculty in Chemistry in partial fulfillment of the requirements for the degree of Doctor of philosophy, The City University of New York.

1974

This manuscript has been read and accepted for the Graduate Faculty in Chemistry in satisfaction of the dissertation requirement for the degree of Doctor of Philosophy.

7/9/74
date

Arthur E Woodward
Chairman of Examining Committee

7/11/74
date

Leonard H. Schwartz
Executive Officer

George Odian

Supervisory Committee

The City University of New York

ACKNOWLEDGEMENTS

I would like to take this opportunity to thank my mentor, Professor Arthur E. Woodward, for his valuable time, advice, and guidance during the duration of my graduate years.

At the same time, I would like to extend my gratitude to both Professors D. R. Morrow and G. Odian for their most helpful suggestions.

Abstract

BROAD-LINE NMR INVESTIGATION OF THE AMORPHOUS COMPONENT IN POLY(TRANS 1,4 BUTADIENE) AND POLY(4 METHYLPENTENE 1) CRYSTALS WETTED BY CARBON DISULFIDE

BY

KENNETH S-B ENG

Adviser: Professor Arthur E. Woodward

Crystals of poly(trans 1,4 butadiene) and poly(4 methylpentene 1) were grown from dilute solution in various solvents.

Broad-line nuclear magnetic resonance spectroscopy was carried out in the temperature range from -95^{o} to $-15^{o}C$ on these crystals wetted with a non-protonated liquid, CS_2, as grown and annealed crystals being investigated. Narrow-line to broad-line intensity ratios were calculated employing the straight line approximation technique.

The n.m.r. results suggest that the amorphous segments in CS_2 wetted PTBD and P4MP1 crystals are under varying degrees of restraint. For crystals with approximately the same thickness, the crystallinity and the nature of the amorphous component for PTBD and P4MP1 crystals were found to depend upon the growth solvent, crystal morphology and the thermal history. The crystalline content increased upon annealing PTBD crystals at $80^{o}C$, a temperature above the crystal transition

temperature. On the other hand, annealing at 150^{o}C and above leads to a decrease in crystalline content in P4MP1 crystals accompany with relief of restraints in the stressed amorphous regions.

Some crystal dissolution results suggest that for PTBD and P4MP1 crystals a mosaic structure exists.

TABLE OF CONTENTS

LIST OF FIGURES

LIST OF FIGURES (cont'd)

LIST OF TABLES

INTRODUCTION

POLYMER CRYSTALS - GENERAL REMARKS

The formation of single crystals of polymers was observed during polymerization as early as 1919.[1-4] In 1957, the growth of such crystals from supercooled dilute polymer solution was reported.[5-7] The discovery that single crystals of polyethylene, and other polymers can be grown from dilute solution has stimulated great interest in the nature, and properties of these formations. The interest arises not only for the solution grown structures themselves, but also for their significance in the study of polymers crystallized from the melt. The aspect of the solution grown crystals that has received the greatest attention is their morphology.[8]

All polymer single crystals grown from dilute solution have the same general appearance, being composed of thin flat or nearly flat lamellae. These lamellae are about 100 Å thick depending upon the degree of supercooling,[8] and many microns in lateral dimensions depending upon the crystallization conditions, such as polymer dissolution temperature.[9] X-ray and electron diffraction[8, 10-12] investigations support the view that the long axes of the polymer molecules in such crystals are approximately perpendicular to the large upper and lower surfaces. Since the polymer molecules are known to be much longer than 100 Å, the startling but nevertheless definite conclusion was reached that the upper and lower surfaces consist of chain folds. Two different theories

describing the formation of single polymer crystals from dilute solution have been given. One, being developed by Peterlin, Fischer, and Reinhold,[13-16] suggests that the fold period is determined thermodynamically. The other theory which is base upon a kinetic approach was given independently by Lin, Price, Lauritzen and Hoffman.[17-20]

From the very beginning, according to the diffraction evidence, and by more detailed inspection of the morphology, some workers[21-24] claimed that polymer single crystals were perfectly regular crystalline entities. Thus, the faces of these crystals containing the chain folds were believed to be regular, and the fold lengths to be uniform to a high degree, varying slightly about some mean value.[25] However, it is clear that morphological studies are inherently limited with respect to providing information at the molecular level. Arguments were also presented in favor of the random irregular switchboard polymer chain re-entry, and the loose loopy amorphous fold surface by Fischer and Lorenz,[27,28] Jackson et. al.,[29] and Flory.[26,30] These authors based their conclusions on the determination of the density of single crystal mats of polyethylene. However, Kawai and Keller[31] obtained density data using a pycnometer which supports the regular crystal model.

Later, attempts were made by Peterlin, and Keller, and their co-workers[32-32,59,67] to study polyethylene crystals by degrading the amorphous portion with fuming nitric acid at high temperature (85°C). The interpretation of their data was

based on the assumption that the uncrystallized regions are more accessible to the acid, and to oxidation, so that after a while only the well-crystallized crystal cores are exposed, and all the amorphous regions of the crystals are destroyed. The initial rate of weight loss, N.M.R. intensity ratio, N.M.R. second moment, heat of fusion, density of the crystals, molecular weight distribution by gel permeation chromatography (GPC), and X-ray diffraction were measured as functions of the time of acid treatment. The rate of degradation was found to take place in two stages: It was assumed that during stage I, the fast stage, the amorphous surfaces of the crystals are destroyed, and during stage II, the slow stage, nitric acid penetrates into the crystal interior, and the reaction rate decreases. More than 50% amorphousness was found for polyethylene single crystals. More recent work by Keller and co-workers[35,36] revealed that the experiments involving fuming nitric acid led to erroneous conclusions. It was found that the crystal core is also attacked and thinned by the acid, and the slowing down of the reaction during stage II was due to accumulation of the reaction products. These more recent studies were based on the molecular weight distribution as followed by gel permeation chromatography during the course of degradation by dilute nitric acid, and ozone. Keller, et. al.[35,36] suggested that the single polymer crystal consists of a comparatively perfect central core with a gradual increasing number of terminating folds as the surface is approached. This implies

that, in the surface region, the density is decreasing on going outward from the interior.

A number of infrared absorption bands have been studied by Brown,[37] Koenig, and Witenhafer,[38] and Koenig, and Hannon[39] to determine their possible connection with the fold surface. Krimm and Bank[40,41] have concluded, based on an infrared study of the 71 cm^{-1} absorption for polyethylene single crystals consisting of a mixture of normal, and deuterated hydrocarbons, that there is an adjacent re-entry fold on the surface. Kawai, Goto, and Maeda[42] support this hypothesis as a consequence of their results from a study of the molecular weight dependence of crystallinity and surface structure. Okada and Mandelkern[43] reported that their studies of polyethylene single crystals using infrared spectroscopy support the concept of a disordered amorphous surface. From the determination of the long spacing change by swelling the polyethylene single crystals with a liquid, Udagawa, and Keller[44] have also found this disordered amorphous layer along the fold surface which expands by swelling. However, a conflicting conclusion was obtained, based on the infrared intensity ratio of the 1340cm^{-1}/1350 cm^{-1} absorptions, by Schonhorn, and Luongo.[45] They concluded that the surface structure of polymer single crystals is somewhat between an amorphous and a tightly folded structure.

Based on the discussion above, it is clear that, in spite of the large number of investigations that have been carried

out on polyethylene, work on crystals grown from other polymers was needed in order to understand the more precise structure and the nature of the amorphous, as well as the crystalline regions.

For that reason, a series of investigations was started by Woodward and co-workers on poly(trans 1,4 butadiene), PTBD.[49,53,73,83] These studies and other pertinent ones are reviewed in the following section.

PTBD SINGLE CRYSTALS

The crystal structure of the low temperature form of PTBD was given by Iwayanagi et. al.[78] by X-ray analysis. It belongs to the monoclinic system with the space group $P2_1/a$. The unit cell with the lattice constants, a=8.63 Å, b=9.11 Å, c=4.83 Å, and $\beta=114^{\circ}$, includes four molecular segments. The arrangement of the four molecules in the unit cell projected on the three planes perpendicular to the a-, b-, c-axes are shown in Figure 1a, Figure 1b, Figure 1c, respectively.

It has been reported that PTBD undergoes a reversible first order solid-solid phase transition.[80] The low temperature form is designated Form I and the high temperature form is Form II. Stellman et. al.[83] found that the high temperature form of PTBD crystals has a very slowly rising heat capacity, indicating that many of the available conformational states are accessible. This implies that a high degree of conformational freedom exists in the high temperature form of the crystal.

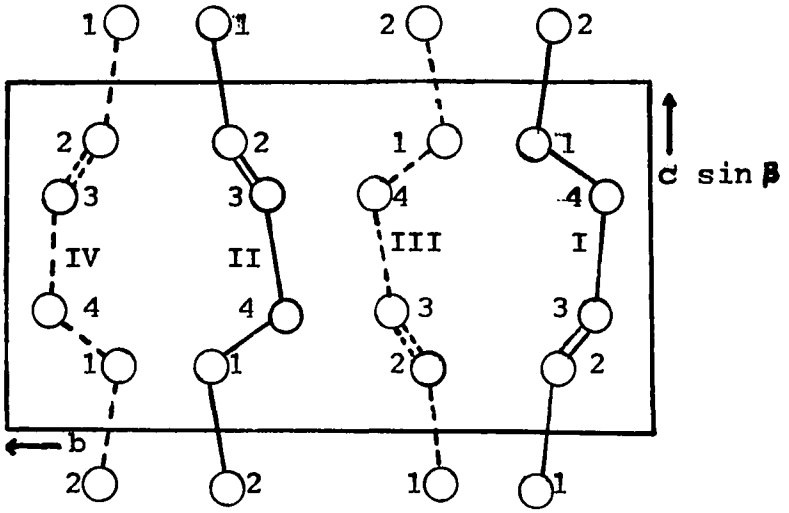

Figure 1a. Arrangement of the four molecules of PTBD in the unit cell projected on the plane perpendicular to the a-axis. The chemical bonds of the rear molecules are shown by broken lines.[78]

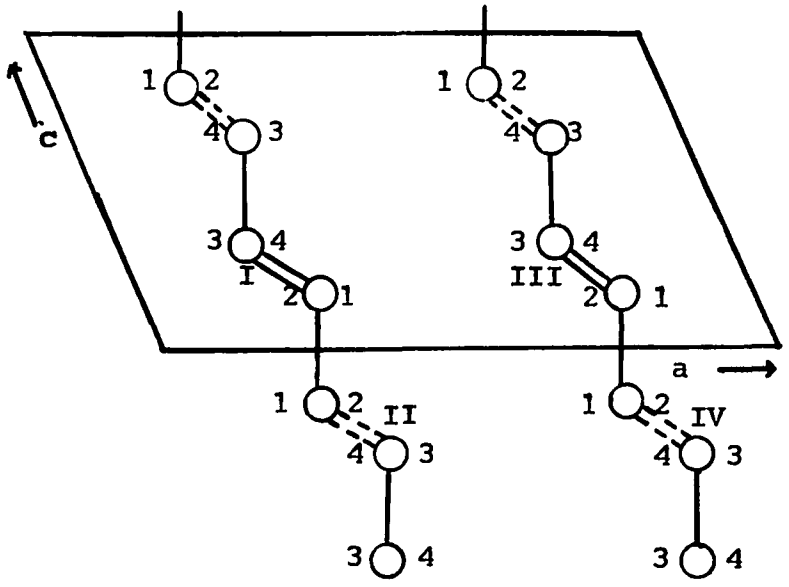

Figure 1b. Arrangement of the four molecules of PTBD in the unit cell projected on the plane perpendicular to the b-axis.

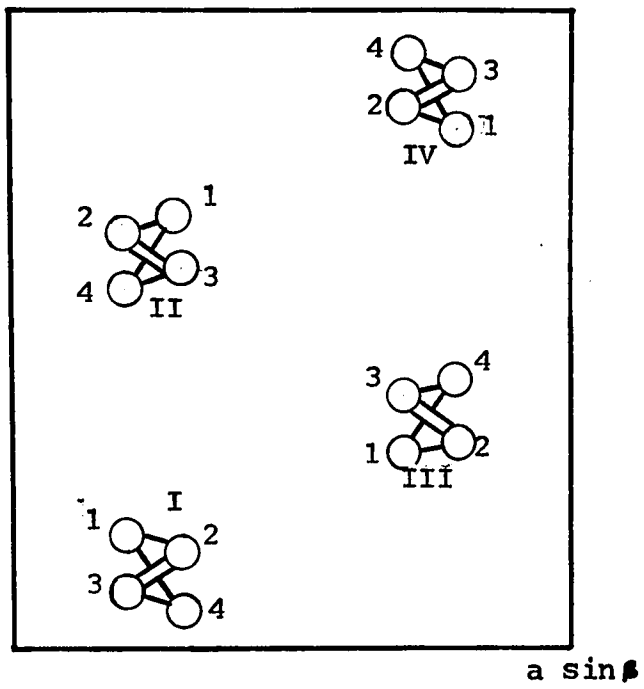

Figure 1c. Arrangement of the four molecules of PTBD in the unit cell projected on the plane perpendicular to the c-axis.

It has been reported that poly(trans 1,4 butadiene) crystals grown from different solvents have different numbers of double bonds available for reaction,[72-75] differences in infrared spectra,[49] as well as differences in dynamic mechanical behavior[76,77] and thermodynamic properties.[53]

Unlike polyethylene, PTBD is an unsaturated polymer which has a double bond in each repeat unit. Quantitative chemical assay on PTBD crystals was carried out by Stellman and Woodward by epoxidation of the double bonds in crystals suspended in benzene at 6°C.[73,74] The crystals were originally grown from a number of solvents. It was found that depending on the crystal growth conditions from 14-27% of the double bonds are available for reaction with metachloroperbenzoic acid for crystals of approximately the same thickness.[49,53,72,73] This leads to an average value of 2½ monomer units per fold for heptane grown crystals to 5 monomer units per fold for benzene grown crystals. Using the crystal structure given by Iwayanagi et. al.,[78] it was found that tight adjacent re-entrant folding would involve 1.5-2 double bonds per fold. This means that folding in PTBD crystals has some looseness.

The infrared spectra were found by Hendrix, Whiting, and Woodward, to yield a regularity band (1335 cm^{-1}), and an amorphous band (1350 cm^{-1}).[49] The ratio I_{1350}/I_{1335} was found to vary from 1.3 to 0.1 with the solvent, and the PTBD polymer used for the crystal preparation, as well as with thermal his-

tory. I_{1350}/I_{1335} is larger for crystals grown at temperatures below the transition temperature than those grown near to it. Upon heating the crystals above T_{tr} and subsequently cooling, it was found that the infrared intensity ratio, I_{1350}/I_{1335}, decreases. The values of I_{1350}/I_{1335} for PTBD crystals grown from different solvents, and for the crystals after 80°C annealing are listed in Table I. Differential scanning calorimetric studies on PTBD crystals was carried out by Stellman and Woodward.[53] It was also found that toluene and benzene grown crystals have a greater amorphous content than heptane grown crystals. Assuming that ΔH_t, the heat of transition from Form I to Form II, is proportional to the crystallinity, the crystallinity was obtained for toluene and benzene crystals by taking that for heptane grown crystals as 0.8.

Table II shows a comparison of the crystallinities obtained using the I.R. and DSC methods for PTBD crystals. The lack of quantitative agreement for a given preparation is, at least, partially due to limitations on the two methods employed. However, the trend shown is the same, that is, the crystalline content is lower for crystals grown at temperatures substantially below the transition temperature of 71-74°C than for those grown near it. Using the surface fraction of double bonds, α, which were obtained by epoxidation of the crystals in suspension, a crystalline fraction, $1-\alpha$, can be obtained as shown in column 4 of Table II, assuming that all disorder is confined to the crystal surface and is detected by the

TABLE I

I_{1350}/I_{1335} for PTBD Crystal Mats at 25°C.

Sample	Solvent	I_{1350}/I_{1335} As Prepared	I_{1350}/I_{1335} After 80°C Anneal
PTBD-K	MIBK	0.2	0.2
	Heptane	0.2	0.1
	Toluene-ethanol	1	0.4
	Toluene	1.2	0.6
	Benzene	0.9	0.3
	Benzene cast film	0.3	---
	Melt formed	0.5	---
PTBD-U	MIBK	0.2	0.3
	Heptane	0.3	0.2
	Toluene-ethanol	1.3	0.2
	Benzene-ethanol	1.2	0.3
	Melt formed	1	---

Table II. Comparision of Crystallinities for PTBD Crystals.

Growth conditions	Crystalline fraction ΔH_t	I.R.	$1-\alpha$
heptane ($78^{o}C/63.5^{o}C$)	(.8)	.8	.86
toluene ($50^{o}C/23^{o}C$)	.6	.5	.81
benzene ($52^{o}C/8^{o}C$)	.55	.5	.73

epoxidation technique. Comparison of the 1-α values with the crystalline fraction values from I.R. and DSC reveals that, for some preparations, the total amorphous content exceeded that present at the surface alone. It implies that the amorphous regions can exist in the interior of the crystal.

Tatsumi et. al.[76] have attributed a dynamic mechanical relaxation at -10°C (110 cps) for benzene grown PTBD crystals to motion of the loose folds at the crystal surfaces.

Natta et. al.,[80] and Moraglio, and co-workers[81] reported the crystal-crystal transition for bulk PTBD at 76°C. In single crystals, Takayanagi et. al.[76] found that the same transition can occur at a temperature as low as 55.5°C for benzene grown crystals with the transition temperature depending on crystal thickness.

There are two stages which occur upon heating PTBD crystals to temperatures near melting. The first of these occurs in the 50-80°C temperature range, and is the crystalline transformation, in which the interchain spacing increases,[82] the total lamellar thickness increases,[76] and molecular rotation about the chain axes begins.[72] The high-temperature phase is, thus a paracrystal. Annealing of benzene grown crystals at temperatures in the 50-80°C region leads to the diminution and finally to the disappearance of the -10°C mechanical loss peak. Tatsumi et. al.[36] reasoned that annealing led to fold tightening (see Fig. 2) and therefore the loss process was associated with the loose folds. When the crystal is annealed above 80°C to temperatures nearer the

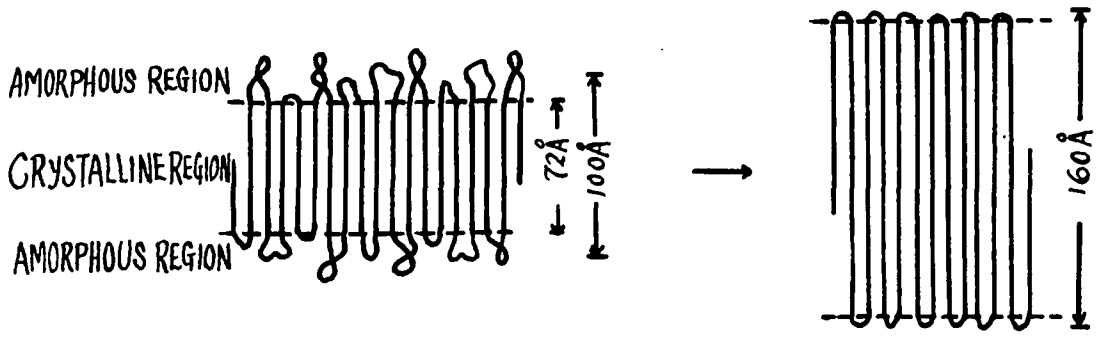

Figure 2. Two-component microcrystalline model of PTBD showing the tightening of loose end loops during annealing.[76]

melting point, then a increase in lamellar thickness can occur and viscoelastic measurements can detect the reappearance of some micro-Brownian motion attributed to loose loops.[76] These authors claimed that a likely possibility for the formation of loose loops was due to the hindering effect of 1,2-(side chain vinyl) impurities which can not be easily accommodated in the crystal component.

It appears that additional studies using different experimental techniques, such as the broad line N.M.R. method, on PTBD crystals would help to further our understanding of the extent of amorphous material and the effect of crystal preparation. Also, it was desired to extend these studies to other polymers. P4MP1 was chosen for studying because this polymer is branched, possessing an isobutyl side chain in each repeat unit,and single crystals of this polymer can be easily obtained from different solvents.

P4MP1 SINGLE CRYSTALS

The crystal structure of P4MP1 was determined by Frank, Keller, and O'Connor,[84] using electron diffraction techniques. More accurate unit cell parameters were determined by Litt[85] from X-ray diffraction studies on drawn fibers. The unit cell is tetragonal, with a=b=18.6 Å, and c=13.8 Å. It was determined[85] that the polymer chains (lying parallel to the c-axis) were helical, with seven monomer units per repeat distance. Steric considerations showed this to be a 7_2 helix. It was also found[85] that the helices were not perfectly regular, but that the true side group symmetry along the helix

was slightly distorted because of interchain crowding. A detailed analysis of the diffraction intensities including forbidden, or absent reflections, provided that the space group $P_{\bar{4}}$, required four fold inversion axes in the unit cell.[85] A unit cell of P4MP1 viewed along the C-axis is shown in Fig. 3. This polymer was more recently studied by Takayanagi, and Kawasaki[47] who found the unit cell parameters to be different depending on the crystal preparation conditions (see Table III).

Earlier studies of isotactic P4MP1 have shown it to have a number of interesting properties. The density and birefringence are practically the same for the amorphous and crystalline phase at room temperature.[86]

Wall and co-workers[107] have attributed the doublet secondary absorption at about -150° to -160°C to thermal motion of the side chain. This secondary absorption for P4MP1 crystals was separated into two peaks by Takayanagi and Kawasaki,[47] who assigned one of them to be associated with the frozen amorphous chains, and the other to be associated with the defect region within the crystalline phase. Their results are shown in Table III. It was found[47] that the crystallinity of P4MP1 crystals is dependent on the crystal growth conditions and thermal history. The crystallinity decreases upon annealing the crystals at 195°C.

The effect of thermal treatment on P4MP1 crystals grown from different solvents was studied by Morrow, Richardson, Kleinman, and Woodward, using the electron microscope, and

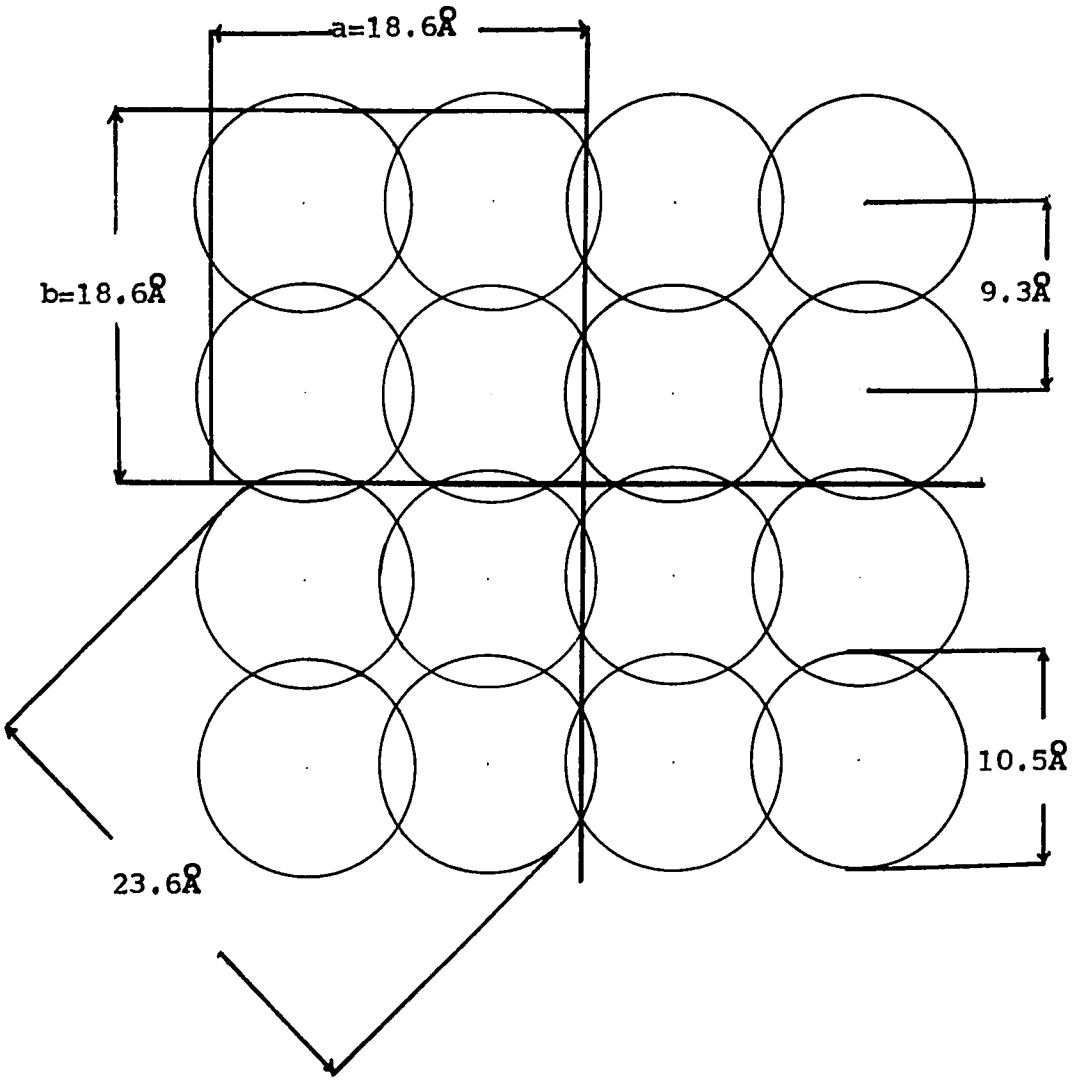

Figure 3. Poly(4 methylpentene 1). Four unit cells viewed down the C-axis; 4 chains per unit cell; 28 monomers per cell; $\rho_{calc.}$=0.830g/cc.

Table III. X-Ray and Viscoelastic Results for P4MP1 Crystals.[49]

P4MP1 crystal preparations	Cryst. form	Lattice constant a=b, c	Hel.	X-ray dens. g/cc.	X-ray crystal-linity	Viscoelastic crystal-linity
.05% xylene $T_{cr.}=60^{o}C$	tetra-gonal	18.6, 13.8	7_2	.813	.65	.66
melt in .05% xylene sol. drop into water, 25°C	tetra-gonal	19.2 7.12	4_1	.848	.50	.43
.05% xylene $T_{cr.}=65^{o}C$	tetra-gonal	19.4 7.10	4_1	.846	.76	.76

the differential scanning calorimeter (DSC). It was found that the crystals have some morphological characteristics in common, such as a square outline with well-defined faces. Various crystals showed the presence of distinct and characteristic melting points. For the crystals grown from the same solvent, the larger crystal shows a greater stability. The first effects of thermal treatment are the appearance of lines, notches at the edges, and holes. An increase in treatment temperature results in an increase in these effects with the formation of fibrillar structures.

Unlike PTBD, P4MP1 has no easily detectable group for chemical assay. It is difficult to apply the density technique, because the difference of the density of amorphous phase and crystalline phase is too small. Also, the infrared spectrum is complicated and it is not yet possible to apply I.R. to the study of the amorphous component of this polymer. The easiest method to use in order to obtain further information of the amorphous component in the polymer is broad-line N.M.R.. This method is introduced in the following section.

GENERAL INTRODUCTION TO N.M.R.

The birth of magnetic resonance may be said to have taken place in 1938, when Rabi et. al.[100] successfully detected the magnetic resonance of protons with a molecular beam apparatus.

Many nuclei act like charged spinning bodies and produce, because of this spin, a magnetic moment along their axis of

rotation. The magnetic moment for a nucleus of spin I can be expressed in terms of the nuclear magneton by the equation:[101-103]

$$\mu = (ge\hbar/2mc)(I) \qquad (1)$$

Where g is a constant referred to as the nuclear g-factor, e is the charge of the particle, m is the mass of the particle, c is the velocity of light, and $\hbar$ is the Plank's constant over 2π.

When a spinning nucleus which is generating a magnetic moment is placed in a uniform magnetic field H_o, it will tend to align itself with the field. By Newton's laws, this will produce an angular acceleration, so that the nucleus will process like a spinning top (see Fig. 4).

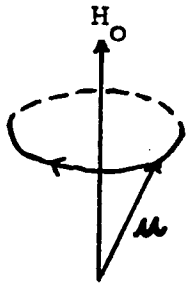

Figure 4. Procession of a magnetic moment μ about an applied magnetic field, H_o. It is assumed that the magnetogyric ratio is positive, as for the proton.[102]

The induced angular velocity of the procession is given by $\vec{\omega} = -\gamma\vec{H}_o$, where γ is referred to as the magnetogyric ratio, $2\pi\mu/Ih$. Thus the Larmor frequency, ν, is:

$$\nu = (\gamma/2\pi)H_o = (\mu/hI)H_o \qquad (2)$$

Where μ=2.79277 Bohr magnetons for proton.

The number of alignments that are possible for a nucleus of spin I, are 2I+1. When a nucleus with I=½, such as a proton, is placed in a uniform magnetic field H_o, it can be regarded as being effectively lined up with the field (when m_I=½), or against it (when m_I=-½), with the former energy state corresponding to the more favorable alignment. This type of splitting of energy levels is referred to as Zeeman splitting (see Fig. 5).

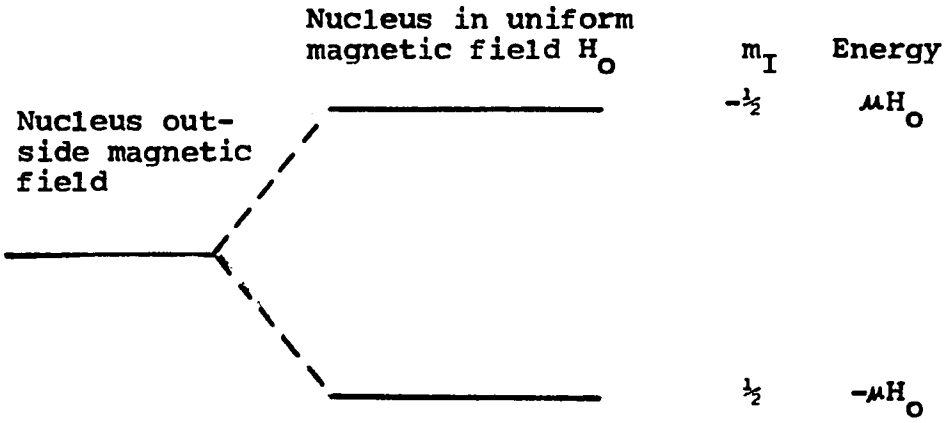

Figure 5. Zeeman splitting of nuclear energy levels for a proton nucleus, I=½.

The energy of each magnetic state is given by:

$$E = -(\mu/I)H_o m_I \qquad (3)$$

Where m_I is the magnetic quantum number, and may have the values I, I-1, I-2, ..., -I.

The basis of the N.M.R. technique is to induce transitions between the nuclear Zeeman levels. To effect these transitions, an alternating magnetic field H_1 is placed in such a fashion that its frequency can be altered conveniently. When the

frequency of H_1 is identical to the processional frequency (see equation 2) of the nucleus being examined, an absorption of energy becomes possible and produces a transition from one energy level to another. According to the quantum mechanically based selection rules, only these transitions are allowed where $\Delta m_I = \pm 1$. The frequency at which this absorption occurs can be calculated using equation 2. When the alternating magnetic field H_1 is at the same frequency as the Larmor frequency of the spinning nucleus, a condition of resonance is said to exist and a transition occurs.

The above discussion is only for an isolated nucleus. In a sample containing a large number of spinning nuclei any nucleus would be subjected to the magnetic field, so that,

$$H = H_o + H_{(due\ to\ neighboring\ nuclei)} \qquad (4)$$

In gases and to some extent in the liquid states, this effect will be averaged out because the molecules are free to move about. In solid samples, however, the nuclear moments are fixed and consequently these interactions do not cancel. This causes a broadening of the resonance absorption over a considerable frequency range at a given magnetic field strength, H_o. Such types of spectra are referred to as broad-line N.M.R. spectra.

BROAD-LINE N.M.R.

The use of the broad-line N.M.R. technique for the study of crystalline polymers began when Wilson, and Pake[104]

separated the absorption line of polyethylene, and polytetrafluoroethylene into two components, the broad line, and the narrow line components, which are associated with the non-mobile and mobile regions of the polymer respectively. The decomposition of the resonance has been carried out in two acceptable ways; the first is known as the straight line method[58,60] and the second one is the low temperature decomposition method.[61,62] The straight line approximation for decomposition of the N.M.R. absorption (see Fig. 6) has been employed to study polyethylene crystals by Collins,[63] McCall and Slichter,[58,60] and Blundell, Keller, and Connor.[34] The low temperature decomposition method was proposed by Rempel et. al.,[61] and Thurn.[62] This method of decomposition is based on the experimental line shape of the broad line component taken at a low temperature (-150^{o}C for polyethylene), at which temperature all the protons are rigid in both amorphous and crystalline regions. In comparison with the straight line approximation, It was found that the low temperature decomposition results in somewhat lower calculated crystallinity (perhaps 2-3% lower).[64] It is expected that broad-line N.M.R. would provide independent information on the amorphous to crystalline ratio in solid polymer in agreement with that from the X-ray method. The lack of agreement between the N.M.R. and X-ray crystallinities has been explained[61] as due to the fact that all the proton in the disordered regions are not in motion during the N.M.R. measurements. To obtain agreement between N.M.R. crystallinity

and X-ray crystallinity, Iwayanagi and Sakurai[65] have employed a different way for line separation for different samples. For dry polyethylene single crystals (precipitated from 0.1% xylene solution at 85°C), the N.M.R. absorption was separated into two components, a broad line, and a narrow line. They found the rigid fraction to compare favorably with the X-ray crystallinity only when the temperature was higher than the primary dispersion temperature. For polytetrafluoroethylene, the N.M.R. crystallinity was obtained by separating the N.M.R, absorption at 74°C into three components. The narrow and the intermediate components were believed to be associated with the amorphous content of this polymer.

It was found previously by Woodward, Odajima. and Sauer[66] that the presence of a low molecular weight liquid can greatly enhance the narrow line component of the N.M.R. absorption while not affecting the broad component for polyolefin polymers. Thus, the swollen specimens can be used to observe the crystalline resonance more clearly. Sorption, diffusion, and other studies[56] have given indirect evidence in favor the view that when a semicrystalline polymer absorbs a low molecular weight substance, the low molecular weight substance enters the amorphous regions only.

Nuclear resonance studies of linear polyethylene that have been swollen by various solvents give direct evidence that this point of view is correct.[64] This experiment consist of equilibrating polymer samples with various amount of a solvent, CCl_4, at room temperature. The mobile fraction

is then measured as a function of solvent concentration. It was found that when polyethylene is swollen by exposure to benzene or some other hydrogen-containing substances, the broad resonance is unchanged, except that the intensity of the narrow resonance increases owing to the presence of the protons in the solvent.

The non-protonated liquid adding method was employed by Blundell, Keller, and Connor[34] to detect the mobilizable material in polyethylene single crystals. The experiment involved the addition of C_2Cl_4 to different samples of polyethylene crystals. The N.M.R. absorption was taken at room temperature. The mobile fractions were obtained using the straight line approximation to separate the broad and narrow lines. It was found that the mobile fraction of the polyethylene single crystals leveled off after initially increasing with increasing the amount of C_2Cl_4 added to the sample. It was also observed for polyethylene that the mobile fraction decreases when the crystal growth concentration was decreased, upon nitric acid treatment of the crystals, or upon annealing the crystals to 121°C. In another study using the N.M.R. technique, Peterlin, Meinel, and Olf[33] obtained the N.M.R. mobile fraction by separating their complicated N.M.R. absorption curve into three components for the elimination of part of the narrow N.M.R. line intensity contributed by the solvent protons. Separation of the N.M.R. absorption into three components was also suggested by Bergmann, and

Nawotki[70,71] for polyethylene swollen in CCl_4. The broad, medium, and narrow component corresponds to rigid, hindered mobile, and liquid-like mobile regions.

STATEMENT OF THE PROBLEM

This investigation had the following objectives. The first objective was to obtain a measure of the amorphous content of polymer crystals containing a non-protonated liquid by the broad-line N.M.R. technique.

Secondly, the effect of the crystallization conditions and of annealing dry crystals on this amorphous content was to be investigated.

A third objective was to study the effect of temperature on the amount of amorphous material available to the non-protonated liquid, CS_2, in the polymer crystals. For the above studies a linear and a branched polymer were employed, poly(trans 1,4 butadiene) and poly(4 methyl pentene-1).

A final objective was to use the N.M.R. results for these polymers plus CS_2 to further our understanding of the organization of the amorphous component in polymer crystals.

EXPERIMENTAL

SAMPLES

Two different polymers were used for these experiments. They were poly(trans 1,4 butadiene), PTBD, and poly(4 methyl pentene-1), P4MP1.

The poly(trans 1,4 butadiene) was obtained through the courtesy of Prof. M. Takayanagi from Ube-Kosan Co., Ltd. of Japan. This polymer was designated PTBD-K by Woodward and co-workers.[49,53,73,74] It was found from infrared analysis, using a Perkin-Elmer 621 spectrometer that this polymer has greater than 95% trans content. A number-average molecular weight of 8670 ($\pm$10%) was found for the as received polymer by DeBell and Richardson Co., using a Hitachi Perkin-Elmer vapor pressure osmometer. For a sample of PTBD-K crystals recovered from n-heptane solution, M_n was found to be 36,900 ($\pm$10%).

The viscosity-average molecular weight M_v was obtained for a PTBD-K using the following relationship derived by R. Endo:[105]

$$[\eta] = 2.9\ 10^{-4} M_v^{0.75} \qquad (5)$$

where $[\eta]$ is the intrinsic viscosity determined by using a Ubbelohde dilution viscometer at 30°C in a chloroform solution.

The intrinsic viscosity and the M_v for PTBD-K was:

$[\eta] = 1.53$ dl/g $\qquad M_v = 92{,}000$

Two different kinds of P4MP1, differing in melt flow index (mfi). were supplied by Imperial Chemical Industies Ltd.

These two polymer are designated as P4MP1(I) and P4MP1(II) whose melt flow indexes are 0.5g/min. and 8.2g/min. respectively when extruded under 5kg presure at 260°C.

CRYSTAL GROWTH TECHNIQUE

Single crystals of poly(trans 1,4 butadiene) and poly(4 methyl pentene-1) were prepared from different solvents employing a growth technique similar to that developed by Blundell and Keller.[59] The procedure involves a minimum temperature of dissolution and self-nucleation.

The crystals of poly(trans 1,4 butadiene) were grown from n-heptane and toluene solvents, using the following procedure. In a 500 ml. Florence flask, the bulk polymer sample was dissolved at the minimum dissolution temperature in a solvent to produce 0.02% solution. Then this solution was filtered through a coarse sintered glass filter, using a water aspirator. When n-heptane was the solvent, the polymer was allowed to precipitate at room temperature. Whenever toluene was the solvent, precipitation was carried out by placing the Florence flask with the solution in an ice bath. The resulting mixtures were re-heated to the original dissolution temperature, and the solution then placed in a thermostated oil bath which was regulated to a constant temperature to within $\pm 0.1^{\circ}C$ until the crystallization process ceased.

The crystals of poly(4 methyl pentene-1) were prepared by a slightly different procedure. A 0.02%, wt.%, polymer-solvent mixture was heated to reflux in a 500 ml. Florence

flask until a homogeneous solution was obtained. Whenever amyl acetate was used as solvent, heating overnight at reflux was necessary to completely dissolve the polymer. With the solution boiling, it was filtered through a paper filter. When amyl acetate was the solvent, the filtrate was kept at room temperature and the polymer allowed to precipitate. Whenever toluene or xylene was the solvent, the filtrate was kept at $0^{o}C$ in an ice bath until precipitation took place. Following this initial precipitation, the resulting mixtures were heated to the minimum dissolution temperature for that solvent-polymer combination. Then the solution was placed in an oil bath which was regulated at a constant temperature to within $\pm 0.1^{o}C$ for crystal growth.

The growth conditions for poly(trans 1,4 butadiene) crystals and for poly(4 methyl pentene-1) crystals are listed in Table IV.

SAMPLE PREPARATIONS FOR N.M.R. MEASUREMENTS

The procedure for sample preparation of PTBD-K crystals for N.M.R. measurement was as follows: The growth solvent (either heptane or toluene) for the crystals was replaced at $-6^{o}C$ by continual addition of CS_2 (spectral grade) in a fine sintered grass filter, using a water aspirator. The mixture of CS_2 and PTBD-K crystals was concentrated via filtration and transferred into the N.M.R. sample tube at $-6^{o}C$ for N.M.R. determinations. Following N.M.R. measurements in the $-24^{o}C$ to $-90^{o}C$ range the samples were dried by directly taking the CS_2 out of the N.M.R. sample tube with the tube immersed

Table IV. Growth Conditions for PTBD and P4MP1 Crystals.

Plymer	Solvent	Dissol. temp.	Rediss. temp.	Growth temp.	Crystal thickness
PTBD-K	n-heptane	78°C	78°C	63.5°C	110±6Å*
PTBD-K	toluene	50°C	50°C	23.0°C	94±3Å*
P4MP1(I)	amyl acetate	165°C	135°C	100.0°C	110±10Å≠
P4MP1(I)	toluene	111°C	90°C	58.0°C	120±10Å≠
P4MP1(I)	xylene	140°C	90°C	60.0°C	120±10Å≠
P4MP1(II)	amyl acetate	165°C	135°C	100.0°C	110±10Å≠
P4MP1(II)	toluene	111°C	90°C	58.0°C	120±10Å≠

* from low-angle X-ray measurement.

≠ from electron microscopy.

in an ice bath using a water aspirator. The temperature of the sample was below -10°C, during removal, due to evaporation. To ensure the complete removal of CS_2, the sample was dried to constant weight. Then N.M.R. measurements were carried out from 25°to -60°C. Following this, the sample was pre-cooled at acetone-dry ice temperature and pre-cooled CS_2 was re-added to the crystals, and N.M.R. measurements were then made at -50°C as a function of time. The heat treated samples were made by removing CS_2 and annealing the dried crystals in a thermostated vacuum oven at 80 ± 0.1°C for 5 hours. After N.M.R. measurements were made from -15° to 25°C on these dried annealed samples, CS_2 was added and N.M.R. measurements were made from -80° to -15°C after equilibrium was attained.

The procedure for sample preparation of P4MP1 crystals was as follows. The crystals were separated from the growth liquid by hot filtration on a fine sintered glass filter and then washed many times with the pure solvent pre-heated to the crystal growth temperature. The crystals were dried in a vacuum desiccator to constant weight. The crystals were then transferred to a n.m.r. sample tube and dried in vacuum until there was no further change in N.M.R. narrow line intensity. N.M.R. measurements were then made as a function of temperature from -42° to 29°C. Following these measurements, the sample was cooled to dry ice-acetone temperature and then pre-cooled CS_2 was added directly to the dried crystals using a dropper. N.M.R. measurements at -50°C were then carried

out on this sample at various times until the narrow line to broad line intensity ratio became constant. Then N.M.R. measurements were made in the -95° to -15°C range for this sample. After these measurements, two samples were chosen, P4MP1(I)(A) and P4MP1(I)(T), to be dried in vacuum and annealed at 150°C for 24 hours; CS_2 was then added and N.M.R. measurements were made at -50°C versus time followed by measurements from -95° to -15°C. For the P4MP1(I)(A) crystals annealing at 200°C and 230°C was also carried out followed by N.M.R. measurements at -50°C, and in the -95° to -15°C region.

BROAD-LINE N.M.R. MEASUREMENTS

The broad-line N.M.R. measurements were made at 90Mhz using a Bruker Model HFX 2/O spectrometer. The narrow line widths were measured at low modulation amplitude (0.3). The N.M.R. absorption were taken at modulation amplitudes seven and ten-fold larger (2.0 and 3.0) to obtain the narrow line and broad line intensities. The relatively larger modulation amplitude was necessary to evalute I_B, the intensity of the broad line component, with reasonable accuracy. It was found that the narrow line to broad line intensity ratio was constant in the modulation amplitude region of 1.5 to 4 at the same temperature.

N.M.R. NARROW-LINE BROAD -LINE SEPARATION

The N.M.R. absorption curves are obtained by integration from the derivative curves in all the measurements. The method for separation was essentially the straight line approximation used by Slichter and McCall,[58,60]

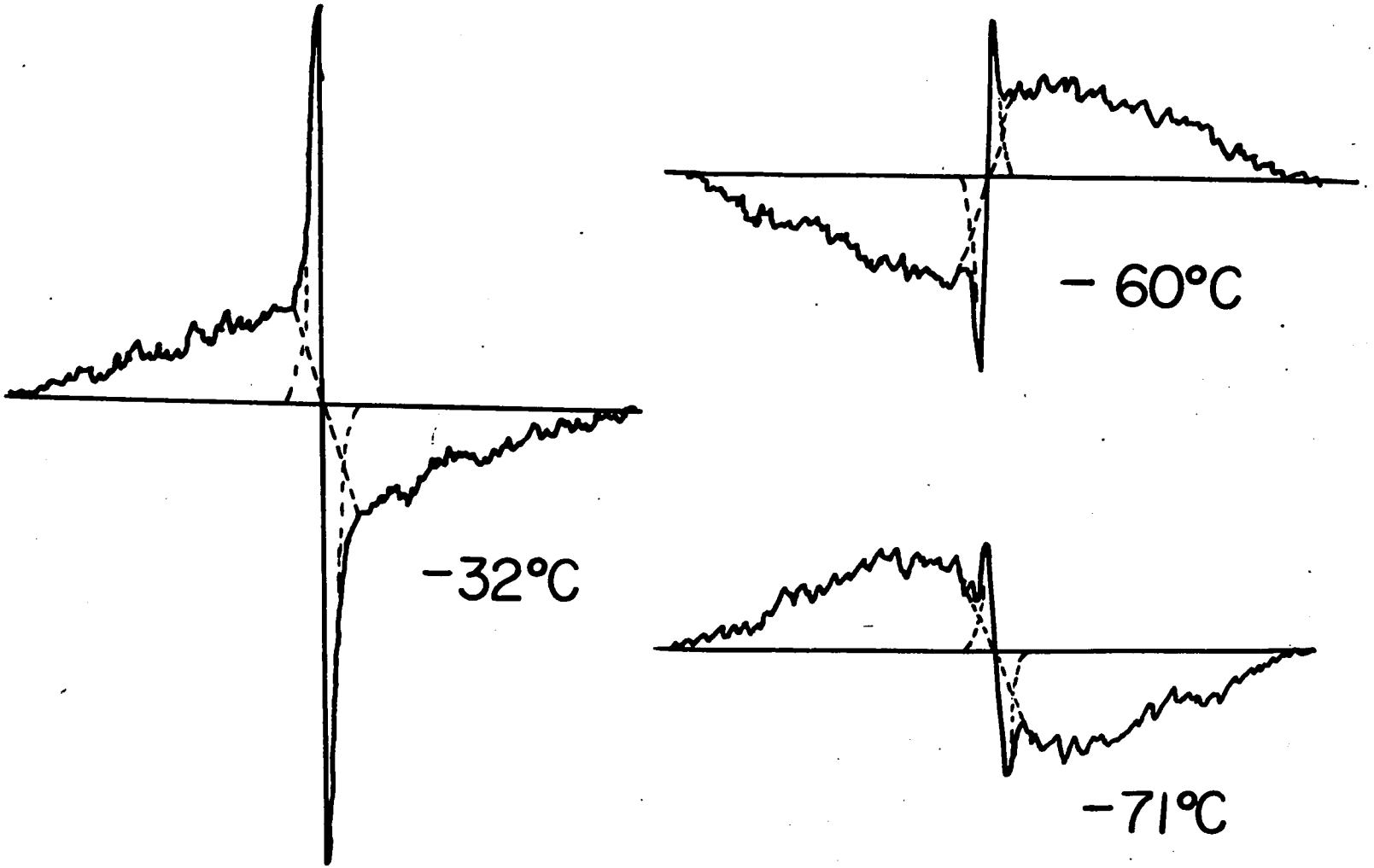

Figure 6. The straight line approximation technique for NMR narrow-line broad-line separation.

and also by Blundell, Keller, and Connor[34] for the measurements of the mobile fraction of polyethylene single crystals.

The separation of the broad-line and narrow-line was effected on the recorded scans by connecting the origin by a straight line with an appropriate point on the envelope. This is illustrated in Fig. 6.

The area under an individual component of the absorption curve is proportional to the abundance of the corresponding phase in the polymer crystals. The narrow component is associated with the amorphous phase, and the broad component is associated with the crystalline phase. The area of each component was estimated with a compensating polar planimeter. The average value of several such area measurements was obtained for each component. The intensity ratio was obtained as the ratio of the area under the narrow line to the area under the broad line component. In all cases, the broad components so obtained corresponded to those found experimentally for the same crystals in the dry state at that temperature.

PRECISION ESTIMATION

Twenty N.M.R. absorption spectra for the CS_2 wetted, 230°C annealed P4MP1(I)(A) sample were obtained at -27°C and twenty n.m.r. absorptions were obtained at -79°C. The intensity ratios were obtained from the absorption curves of these spectra using the compensating polar planimeter employing the straight-line approximation separation technique by two different persons, and the error was obtained comparing the error within each

set of the twenty intensity ratios calculated by two different persons.

For estimating the precision, another crystal sample of P4MP1(I) was prepared separately from amyl acetate employing the same crystal growth conditions, and the N.M.R. measurements were made in the -95^{o} to $-15^{o}C$ region on the CS_2 wetted crystals of this preparation after equlilbrium was attained.

RESULTS

ELECTRON MICROSCOPY

The PTBD crystals grown from n-heptane were regular hexagons as seen in Fig. 7. The crystals grown from toluene were elongated hexagonal crystals (see Fig. 8) and were smaller by a factor of about 2 than those grown from n-heptane. The size of PTBD crystals was found by Stellman[88] to depend on the dissolution temperature; the same effect was reported previously for polyethylene crystals by Blundell and Keller.[9] A typical selective area differaction pattern as obtained from toluene grown crystals is shown in Fig. 9 (the same pattern was obtained from heptane grown crystals). These pattern are in agreement with the structural data[78] obtained by Iwayanagi and co-workers.

The P4MP1(I) crystals grown from amyl acetate were a mixture of regular squares, multiple layers, and regular screw dislocation terraces as can be seen from Fig. 10. The P4MP1(II) crystals grown from amyl acetate were regular single layered squares of uniform size as shown in Fig. 11. The amyl acetate crystals grown from P4MP1(I) polymer were larger by a factor of about 2 than those from P4MP1(II). Both the P4MP1(I) and P4MP1(II) crystals grown from toluene were single layered but of two different sizes as shown in Fig. 12 and 13. The P4MP1(I) xylene crystals appear similar to P4MP1(II) crystals from amyl acetate, but smaller by a factor of 2. A typical field is shown in Fig.14. Electron micrographs of typical fields for the 150^{o}C annealed P4MP1(I)(T) crystals, and the

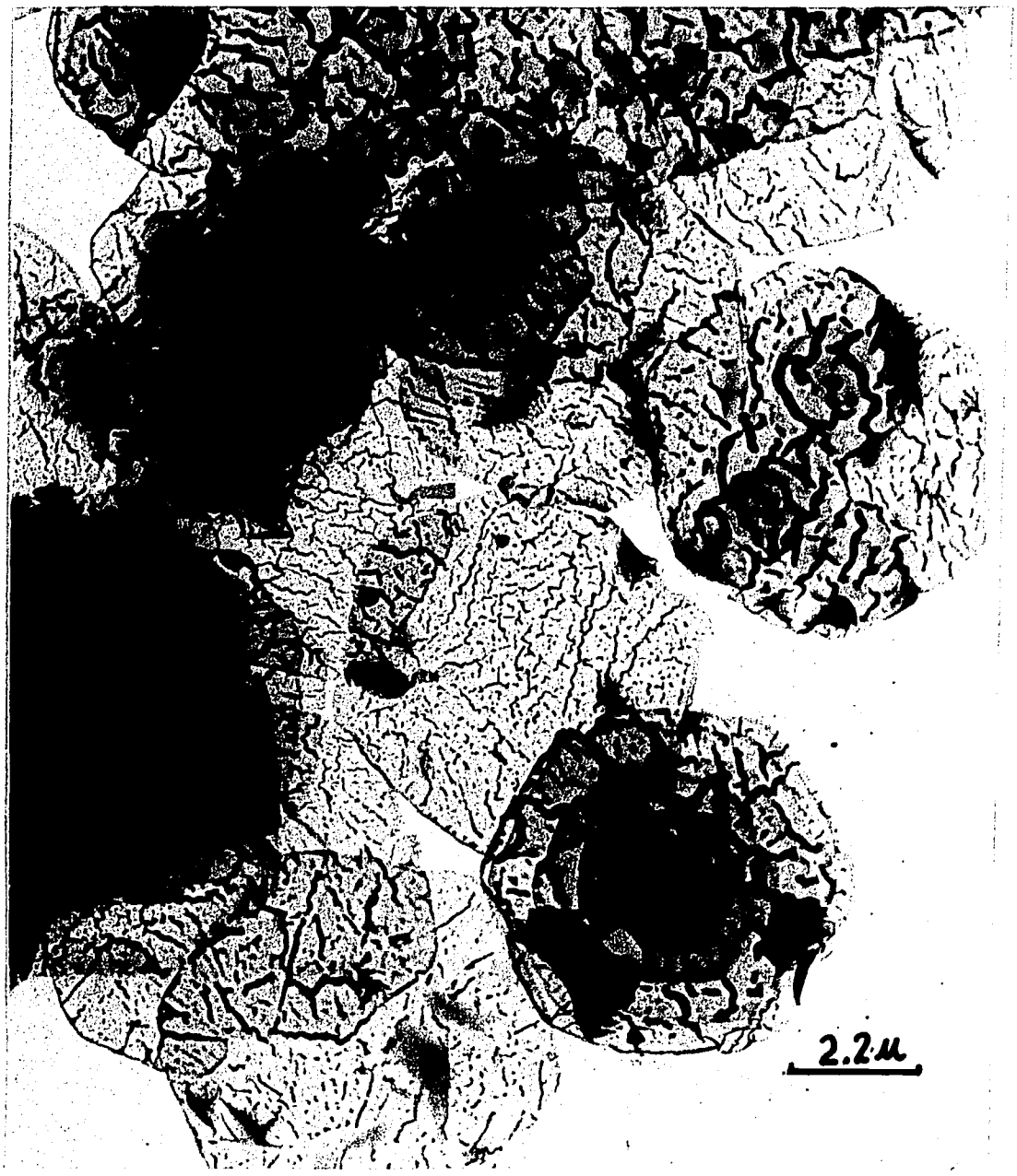

Figure 7. PTBD crystals grown from n-heptane.

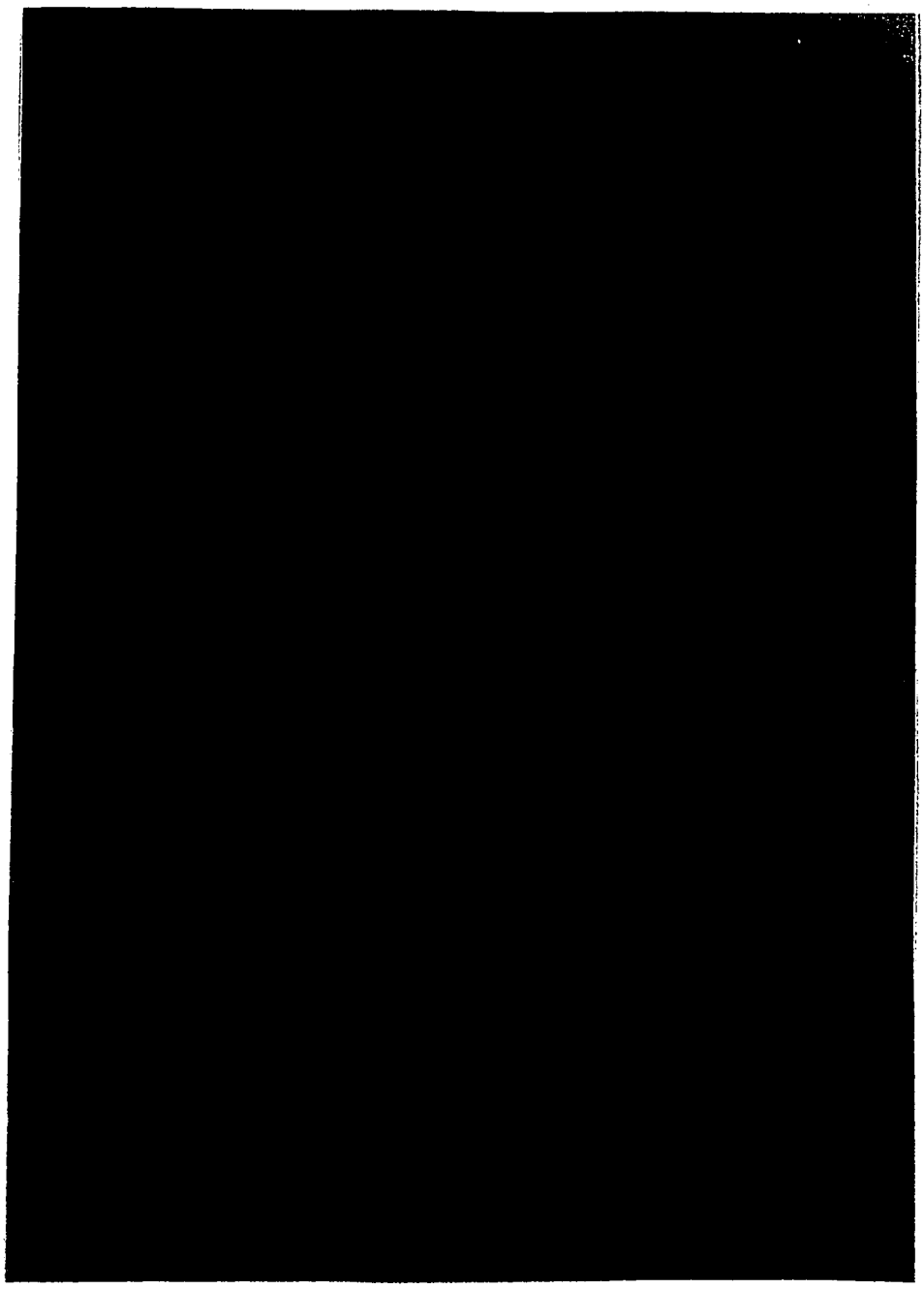

Figure 8. PTBD crystals grown from toluene.

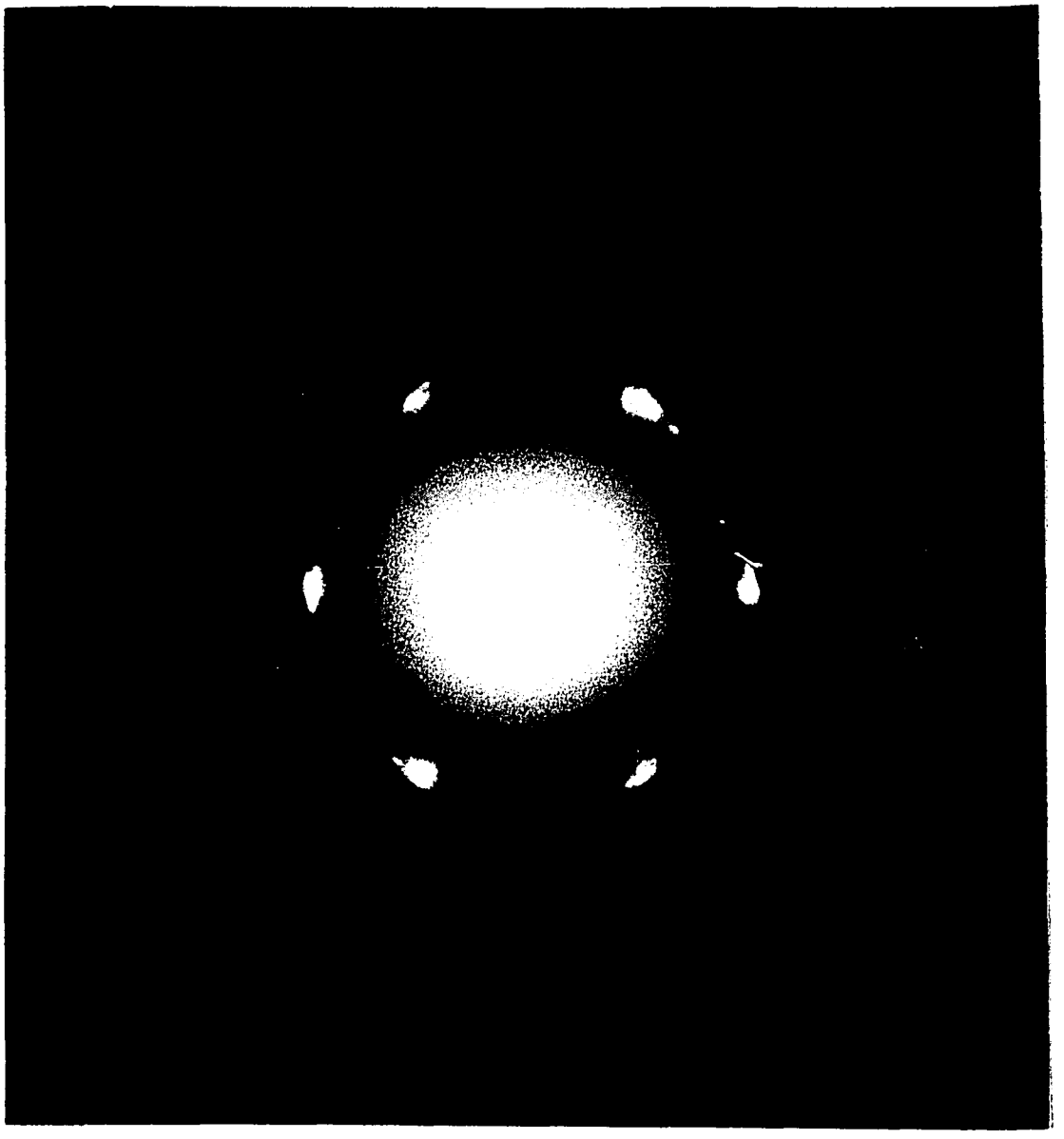

Figure 9. Selected area diffraction pattern for toluene grown PTBD crystals.

Figure 10. P4MP1(I) crystals grown from amyl acetate.

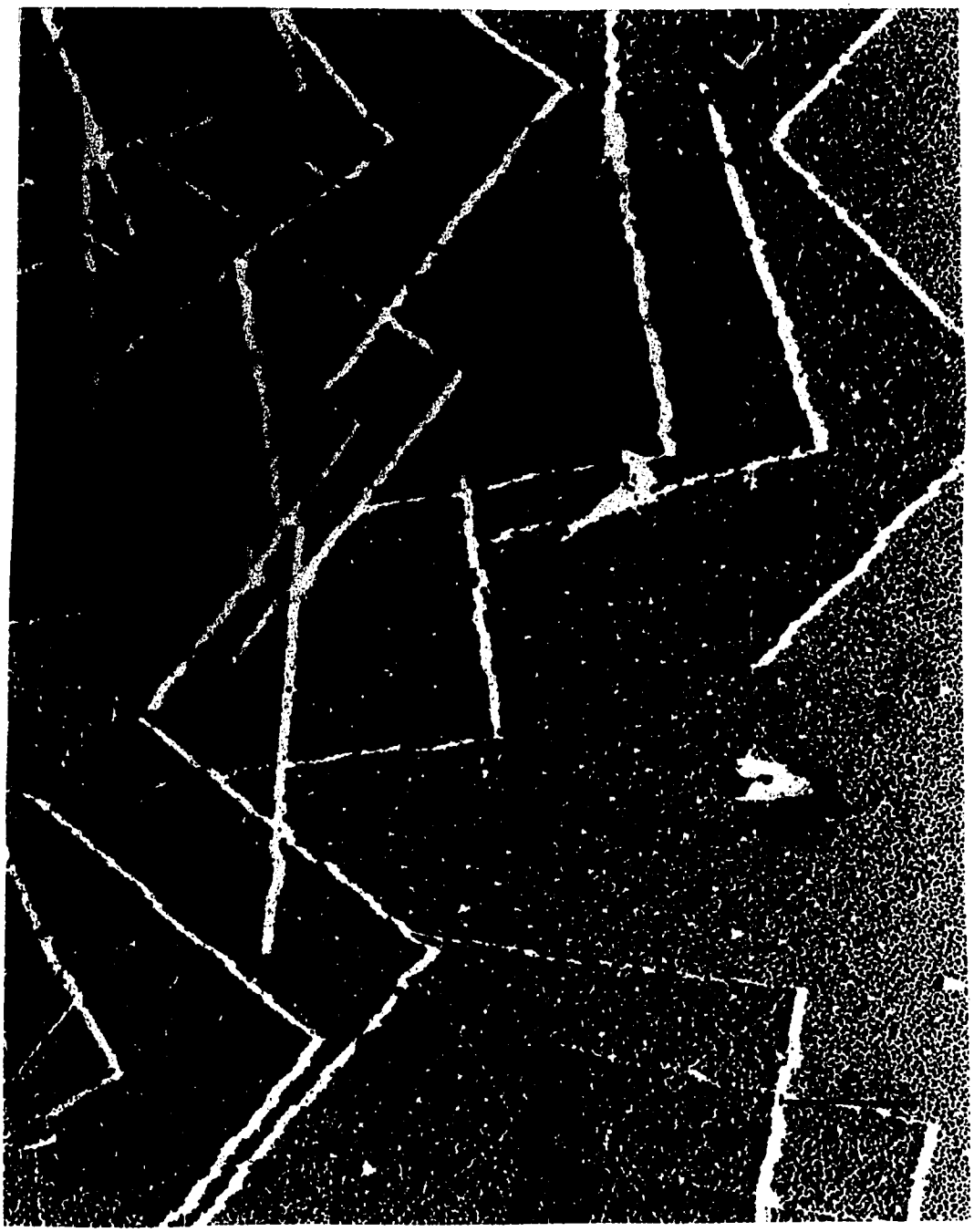

Figure 11. P4MP1(II) crystals grown from amyl acetate.

Figure 12. P4MP1(I) crystals grown from toluene.

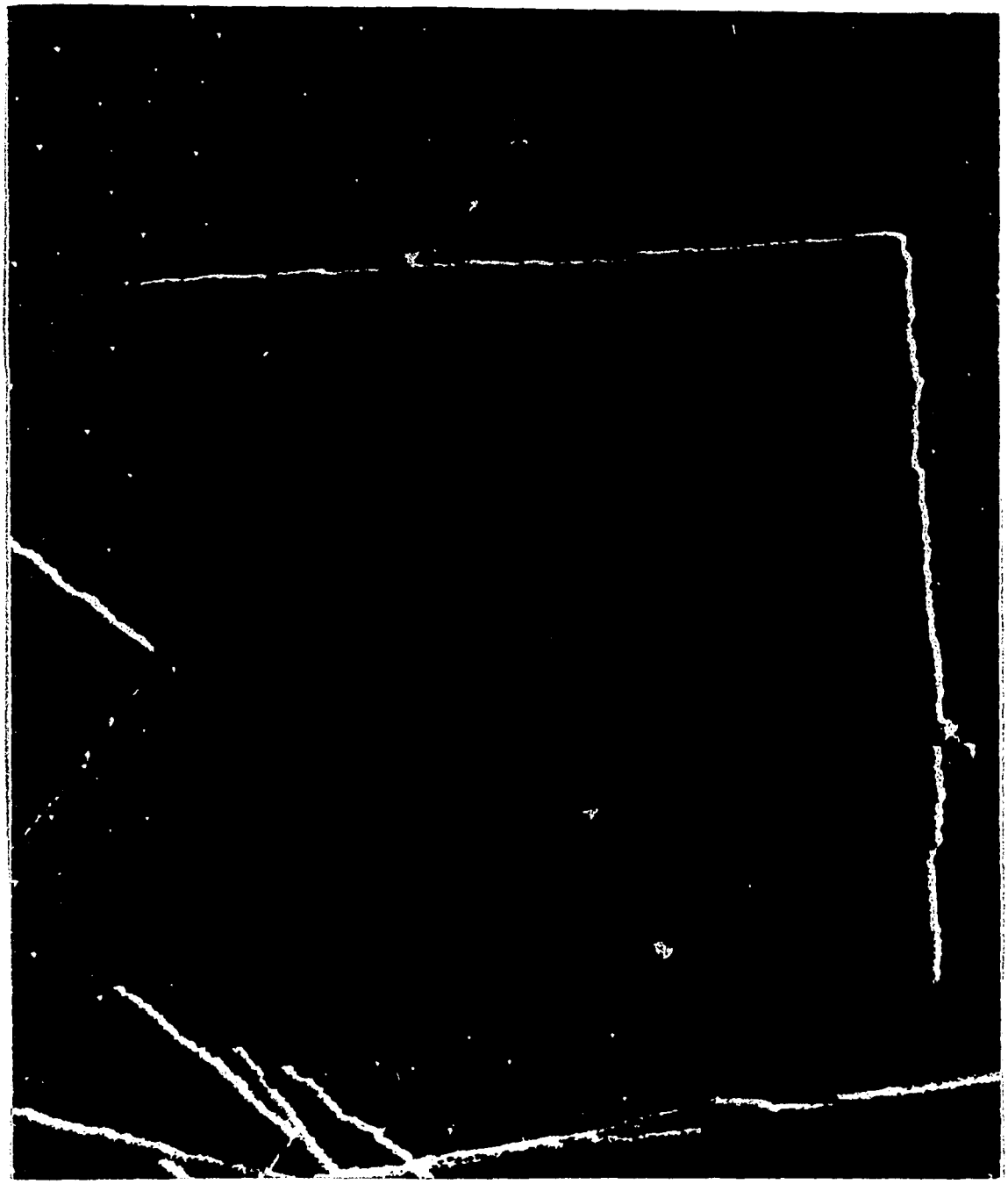

Figure 13. P4MP1(II) crystals grown from toluene.

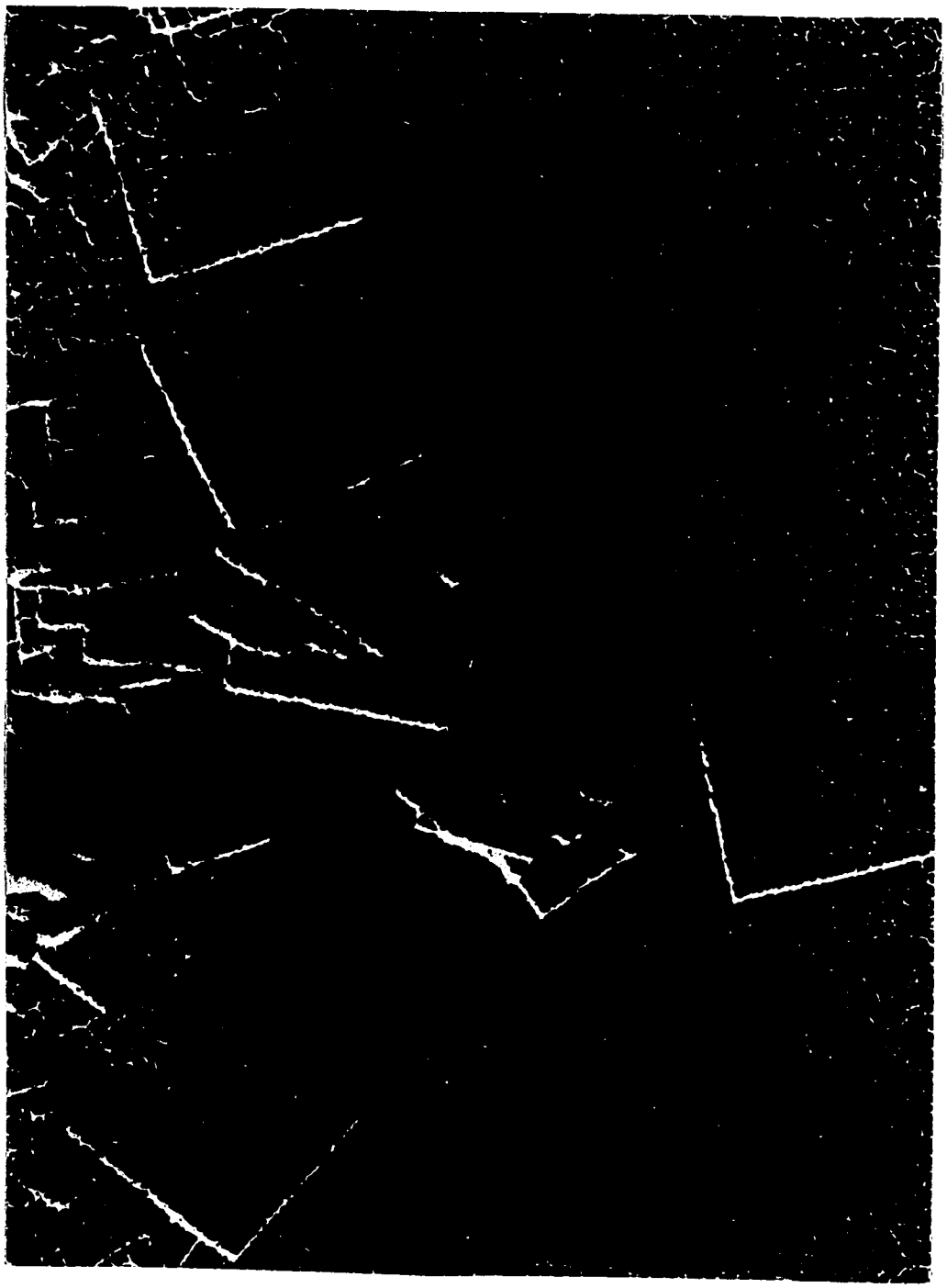

Figure 14. P4MP1(I) crystals grown from xylene.

150°C, 200°C, and 230°C annealed P4MP1(I)(A) crystals are given in Fig. 15,16,17, and 18. Upon annealing at 150°C for 24 hours, there was no change in thickness for both kinds of P4MP1(I) crystals. Only those edges of P4MP1(I) from amyl acetate and of the small crystals from toluene in contact with the carbon film were affected. These affected edges became irregular for amyl acetate crystals, and zigzag-like for the small T crystals. After 200°C annealing, this effect was more pronounced for the P4MP1(I)(A) crystals, with all the edges becoming irregular; the lamellae thickened from 110±10Å to 130±10Å. When the temperature of thermal treatment is increased to 230°C, holes are formed, and the layers of the crystals mesh together with a thickness of 300Å±10Å. It was found previously by Morrow, and co-workers[87] that the selected area diffraction pattern for this sample showed the same tetragonal spacing as those for unheated crystals.

N.M.R. RESULTS FOR PTBD CRYSTALS

The N.M.R. results obtained on dried and CS_2 wetted n-heptane, and toluene grown PTBD crystals are summarized in Figs. 19 and 20. Fig. 19 is a plot of the narrow line-broad line intensity ratio, I_N/I_B, versus temperature. Fig. 20 is a plot of the line width against temperature.

It was found, using electron microscopy, that PTBD crystals grown from n-heptane or toluene but wetted with CS_2 could be stored at temperatures lower than -6°C for over 30 days without noticeable changes. All the N.M.R. results obtained on CS_2 wetted PTBD crystals were at temperatures lower than

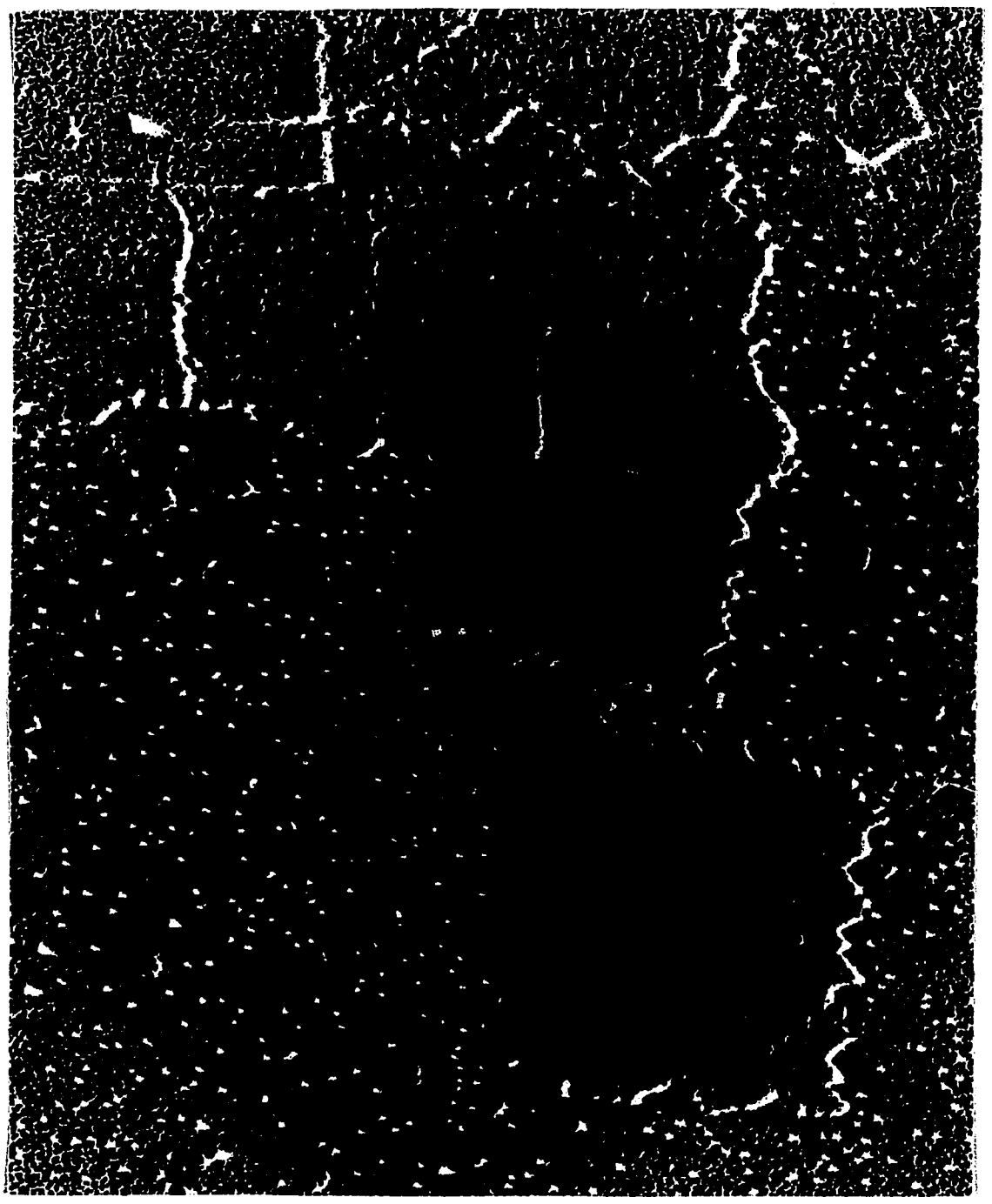

Figure 15. 150^{o}C annealed P4MP1(I)(T) crystals.

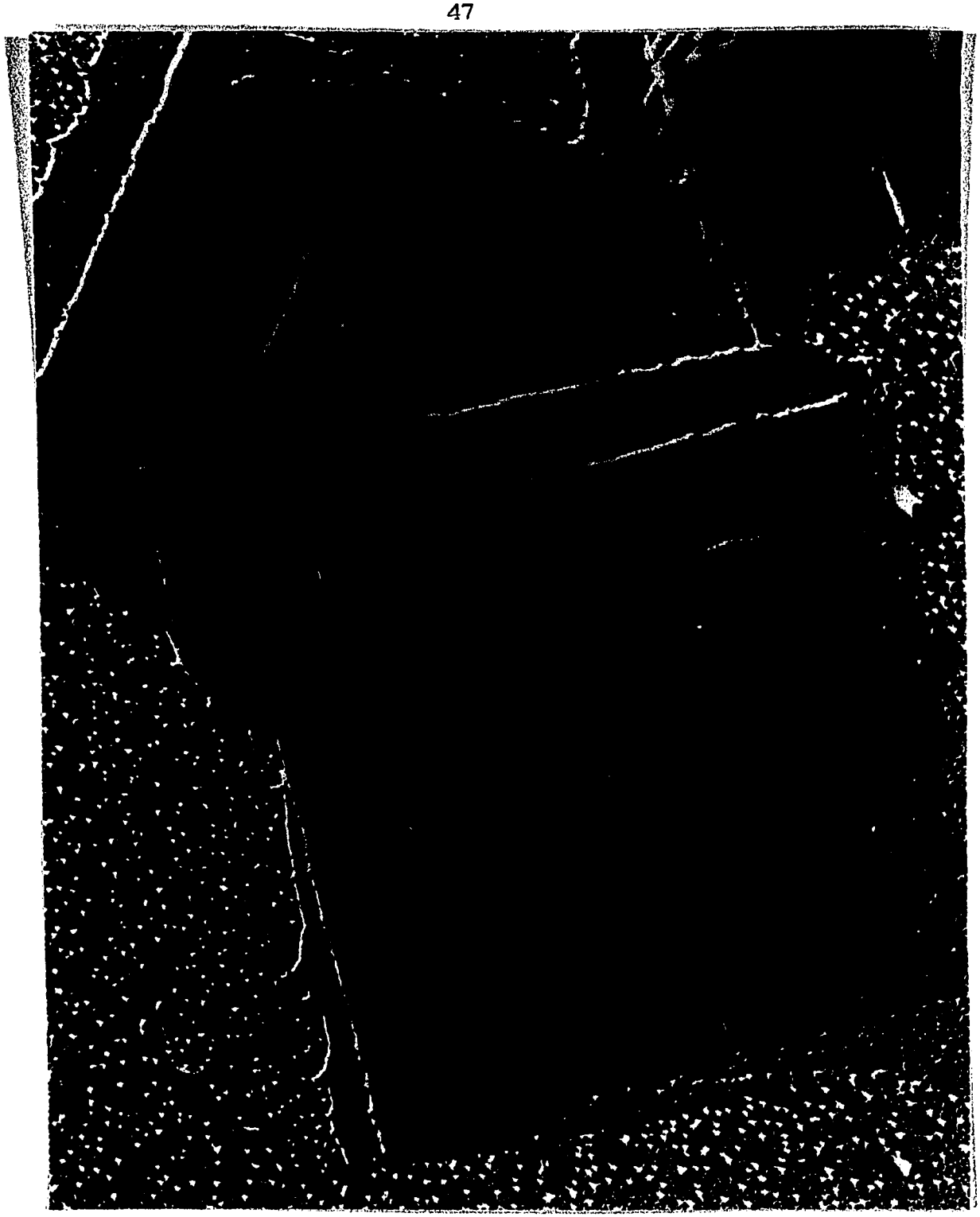

Figure 16. 150°C annealed P4MP1(I)(A) crystals.

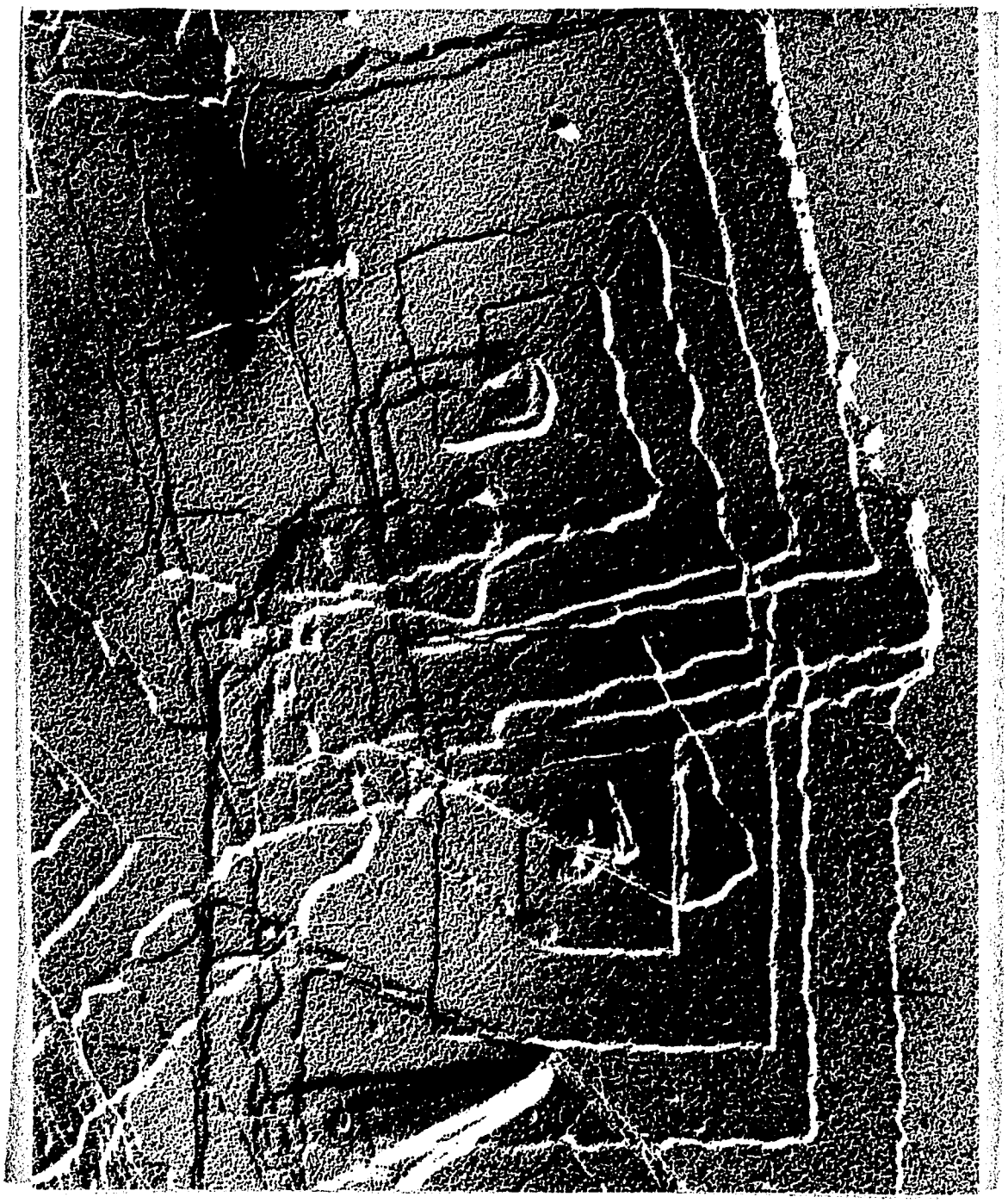

Figure 17. 200°C annealed P4MP1(I)(A) crystals.

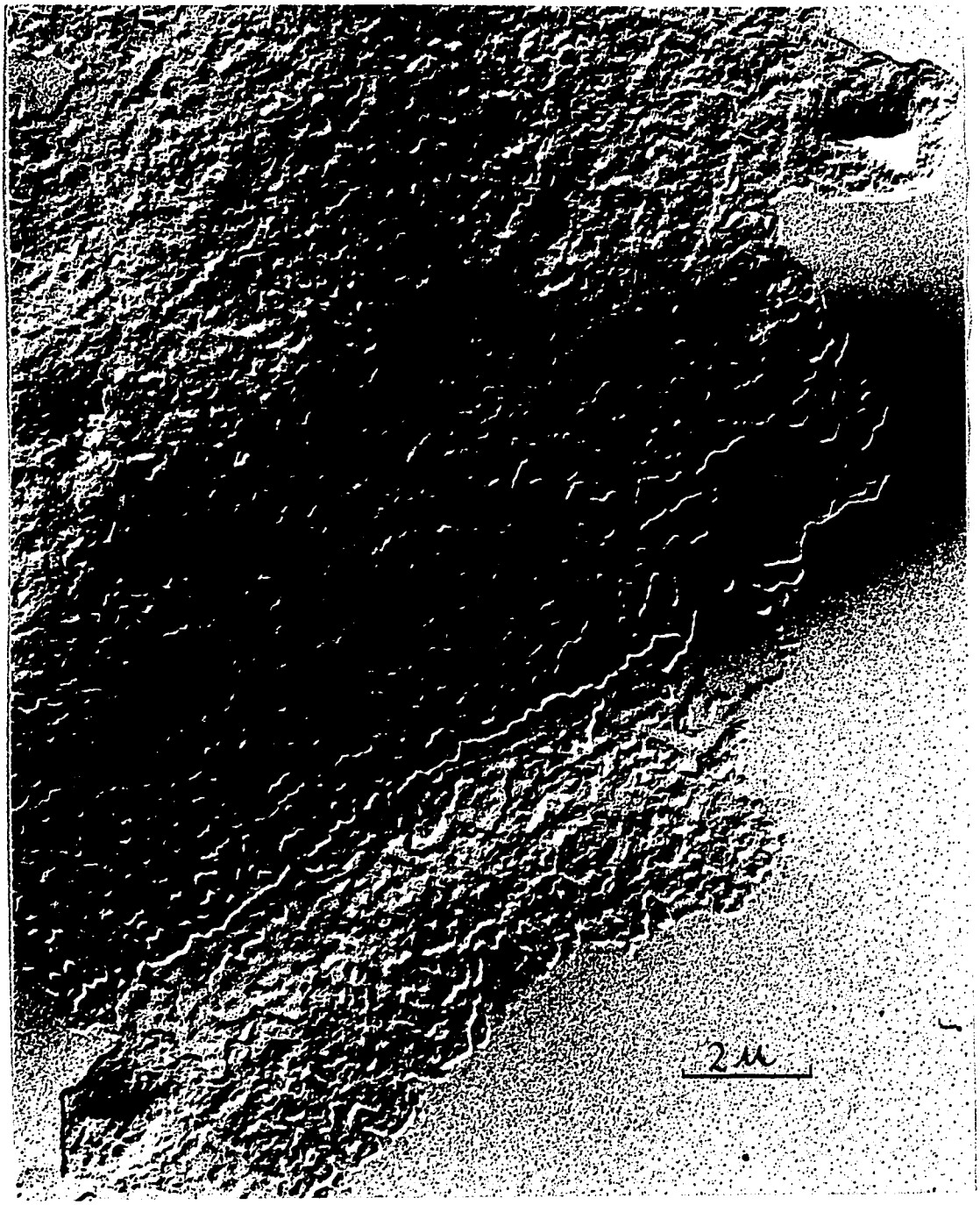

Figure 18. 230°C annealed P4MP1(I)(A) crystals.

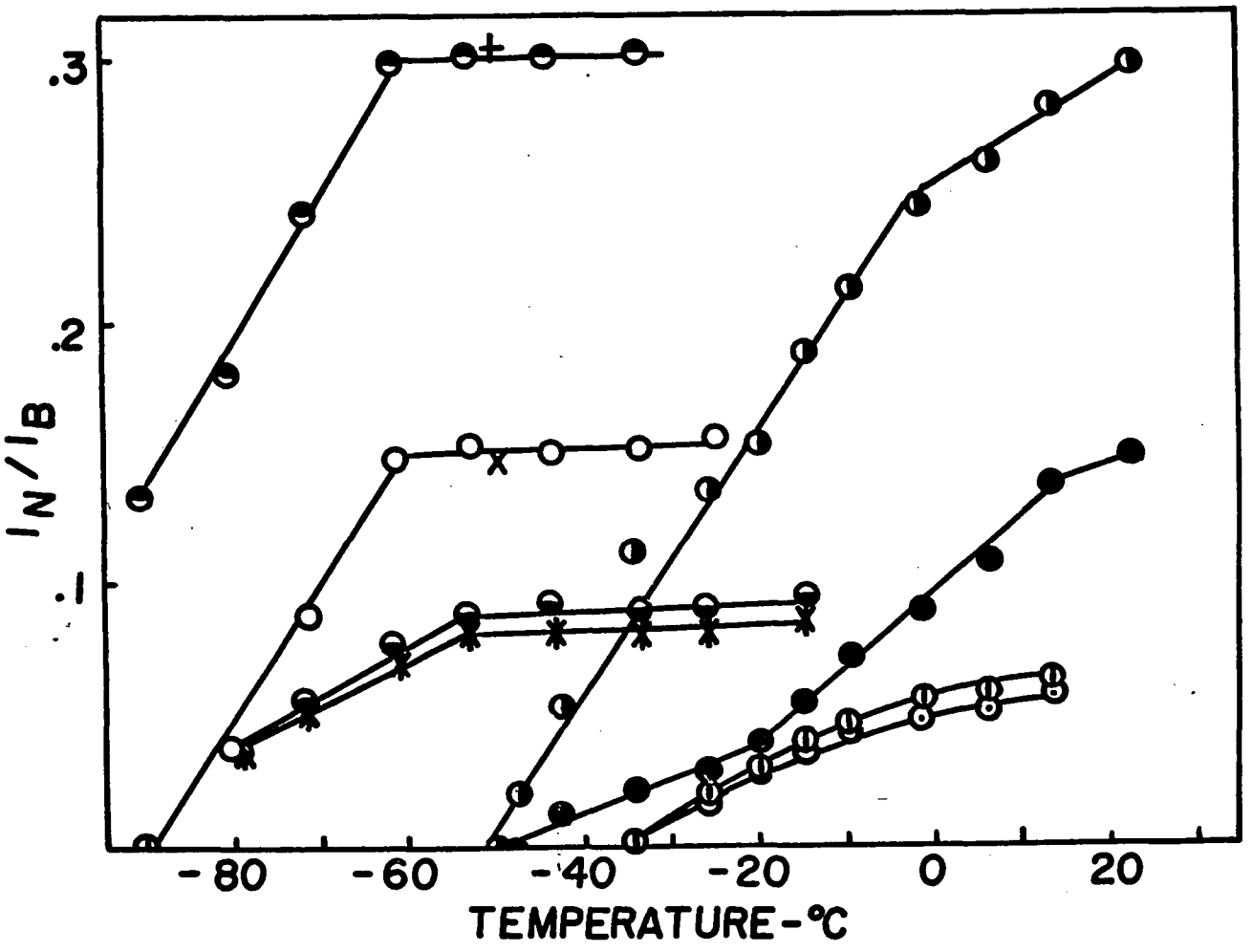

Figure 19. NMR narrow line-broad line intensity ratio vs. temperature for heptane-grown crystals in CS_2 (O), 80°C annealed heptane-grown crystals in CS_2 (✱), dry heptane-grown crystals (●), dry 80°C annealed heptane-grown crystals (⊙), heptane-grown crystals resolvated with CS_2 after 21 min. (X), toluene-grown crystals in CS_2 (⊖), 80°C annealed toluene-grown crystals in CS_2(⊖), dry toluene-grown crystals(◐), dry 80°C annealed toluene-grown crystals(◐), and toluene-grown crystals resolvated in CS_2, after 48 hrs.(+).

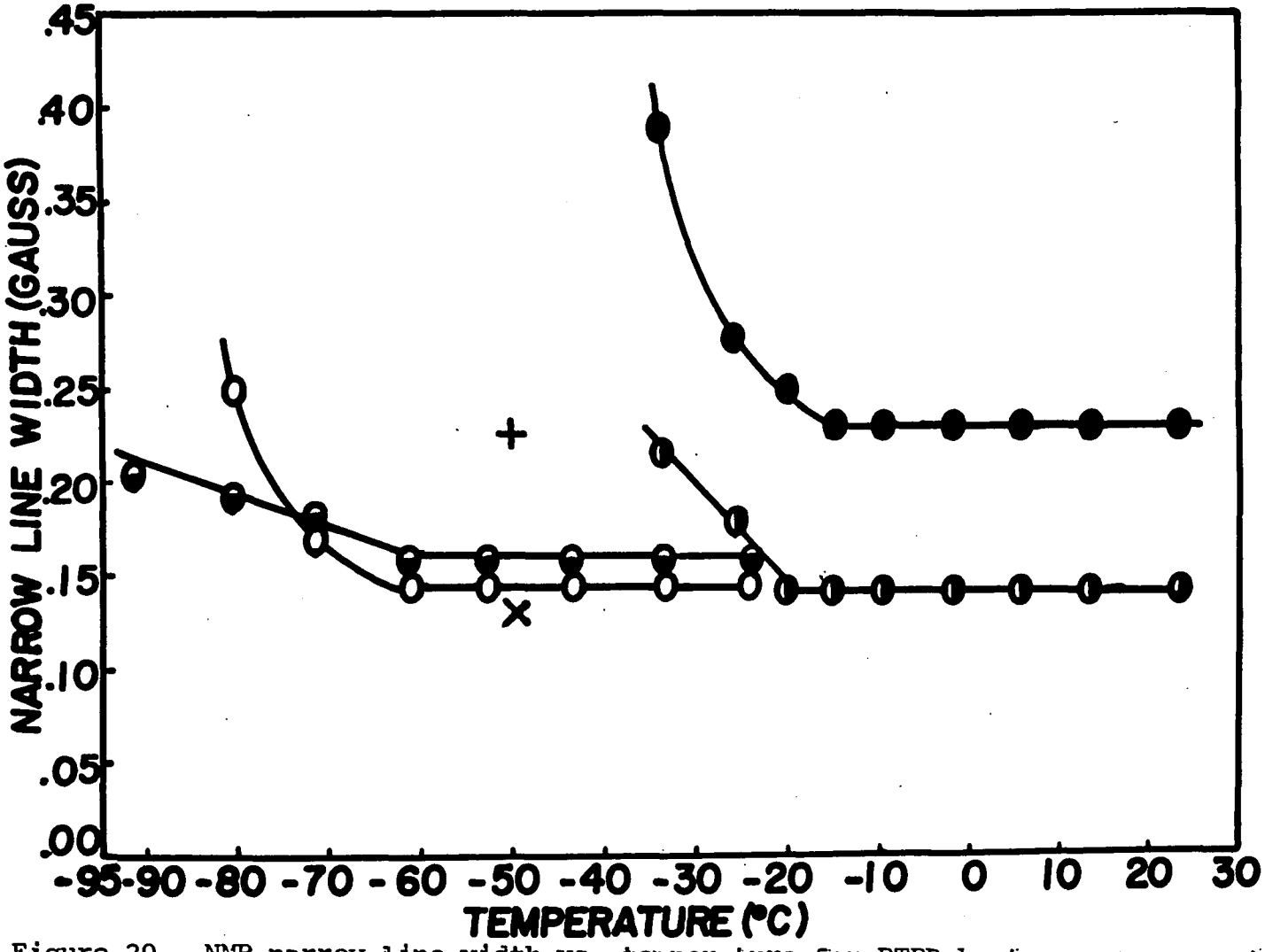

Figure 20, NMR narrow line width vs. temperature for PTBD heptane-grown crystals suspended in CS_2 (O), dry heptane-grown crystals (●), heptane-grown crystals resolvated in CS_2, after 3 min. (X), toluene-grown crystals suspended in CS_2 (⊖), dry toluene-grown crystals (⊖), and toluene-grown crystals resolvated in CS_2, after 90 min. (+).

-10°C. It could be assumed that at the temperatures of the N.M.R. measurements on the CS_2 wetted samples, CS_2 was acting only as a swelling agent for the amorphous parts. The narrow and broad lines were separated employing the straight line approximation.

From Fig. 19, it is found that there is a temperature region in which I_N/I_B is constant for both n-heptane and toluene grown PTBD crystals, provided there is CS_2 present. This temperature region is corresponding to the temperature region in which the narrow line widths remain constant in Fig. 20. The intensity ratio, I_N/I_B, of the CS_2 wetted toluene crystals is greater by a factor of about two than that of the n-heptane grown crystals at temperatures above -60°C. Below -60°C, this factor increases with decreasing temperature.

At -91°C the narrow line of the CS_2 wetted n-heptane crystals has vanished, the narrow line-broad line intensity ratio of the toluene crystals is about .13. The narrow line width of the dried n-heptane crystals is greater than that of the dried toluene crystals by a factor of one-half.

However, the difference in N.M.R. behavior for CS_2 wetted n-heptane and toluene grown crystals disappears after thermal treatment of the dry crystals at 80°C for 5 hours. The intensity ratio is about 0.08 for both CS_2 wetted, 80°C annealed n-heptane and toluene grown crystals.

When CS_2 was added to dry unannealed n-heptane crystals at -50°C, the narrow line width was 0.14 gauss within three

minutes, and it was constant with time thereafter. I_N/I_B for the CS_2 rewetted n-heptane grown crystals was essentially the same as the original CS_2 wetted crystals within twenty one minutes. On the other hand, the narrow line width decreases in value fron about 0.31 gauss at three minutes to 0.22 gauss at 87 minutes, and the narrow line width reached a constant ninety minutes after CS_2 was added to the dried toluene grown crystals. The intensity ratio for toluene grown crystals was 0.26 after one hundred and fifteen minutes, and 0.275 after two hundred and forty seven minutes. The intensity ratio agree with that for the originally wetted crystals within forty eight hours.

The N.M.R. crystallinities of PTBD crystals are listed in Table V.

N.M.R. RESULTS FOR P4MP1 CRYSTALS

Fig. 21 shows a plot of the N.M.R. narrow line-broad line intensity ratio, I_N/I_B, vs. temperature for P4MP1 crystals grown from different solvents.

In Fig. 22 I_N/I_B vs. temperature is shown for CS_2 wetted, 150°C annealed P4MP1(I)(T) crystals, and for CS_2 wetted, annealed P4MP1(I)(A) crystals; the P4MP1(I)(A) crystals were annealed at 150°C for 24 hours and at 200°C and 230°C for two hours.

At - 50°C, the N.M.R. narrow line is absent for the dry crystals of all five preparations; a sizable narrow line component is found in the presence of CS_2.

As found for CS_2 wetted PTBD crystals, there is a temper-

Table V. N.M.R. Crystallinities for PTBD Crystals.

Growth conditions	Thermal history	I_N/I_B (above -60°C)	Crystalline fraction
n-heptane (78°C/63.5°C)	as grown	0.15	0.87
toluene (50°C/23°C)	as grown	0.30	0.77
n-heptane (78°C/63.5°C)	80°C annealed (five hours)	0.08	0.93
toluene (50°C/23°C)	80°C annealed (five hours)	0.087	0.92

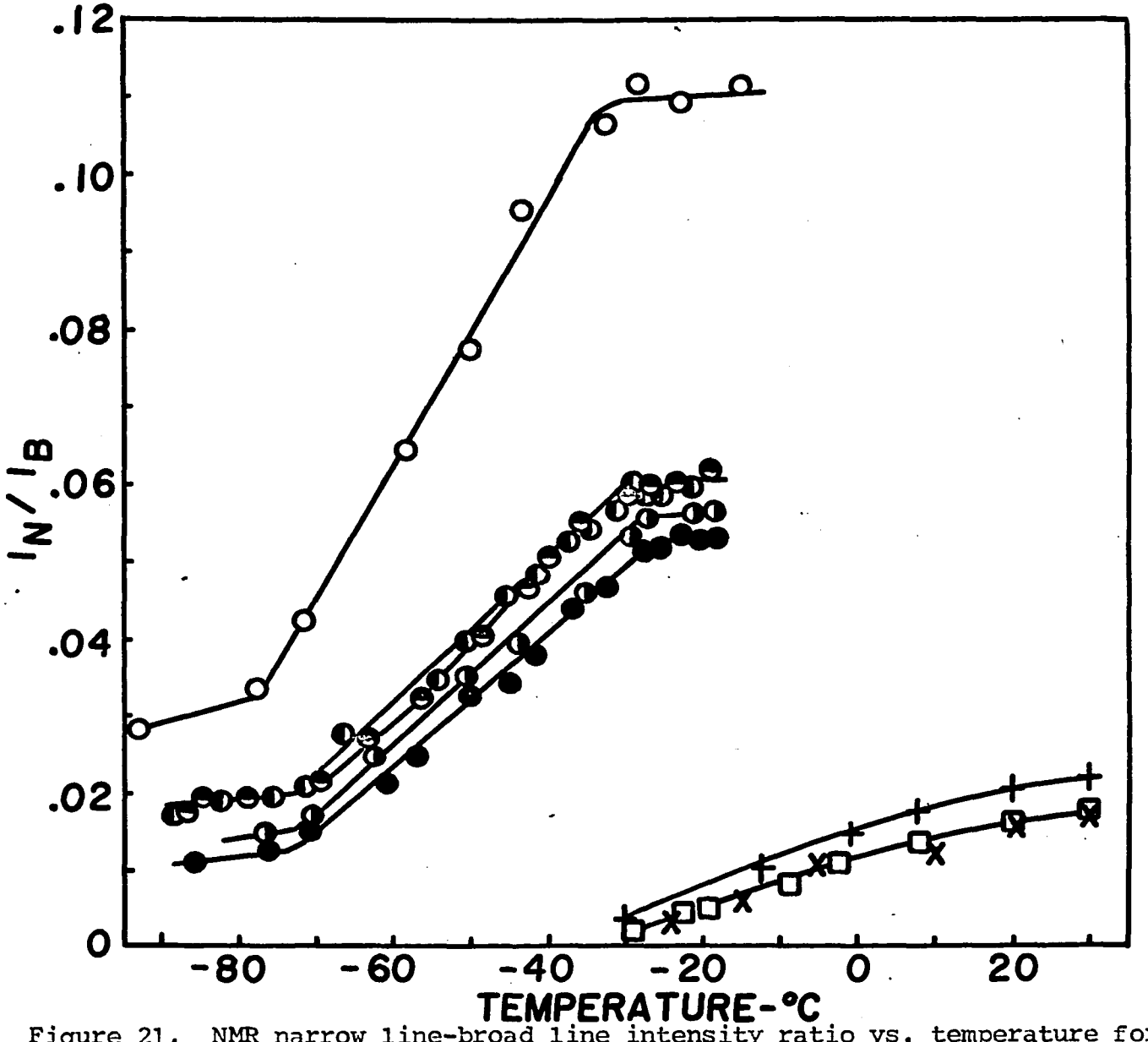

Figure 21. NMR narrow line-broad line intensity ratio vs. temperature for P4MP1(I)(A) crystals wetted with CS_2 (O), dry P4MP1(I)(A) crystals (+), P4MP1(I)(T) crystals wetted with CS_2 (●), dry P4MP1(I)(X) crystals (X), P4MP1(I)(X) crystals wetted with CS_2 (◐), dry P4MP1(II)(A) crystals (□), P4MP1(II)(A) crystals wetted with CS_2(◐), P4MP1(II)(T) crystals wetted with CS_2(●).

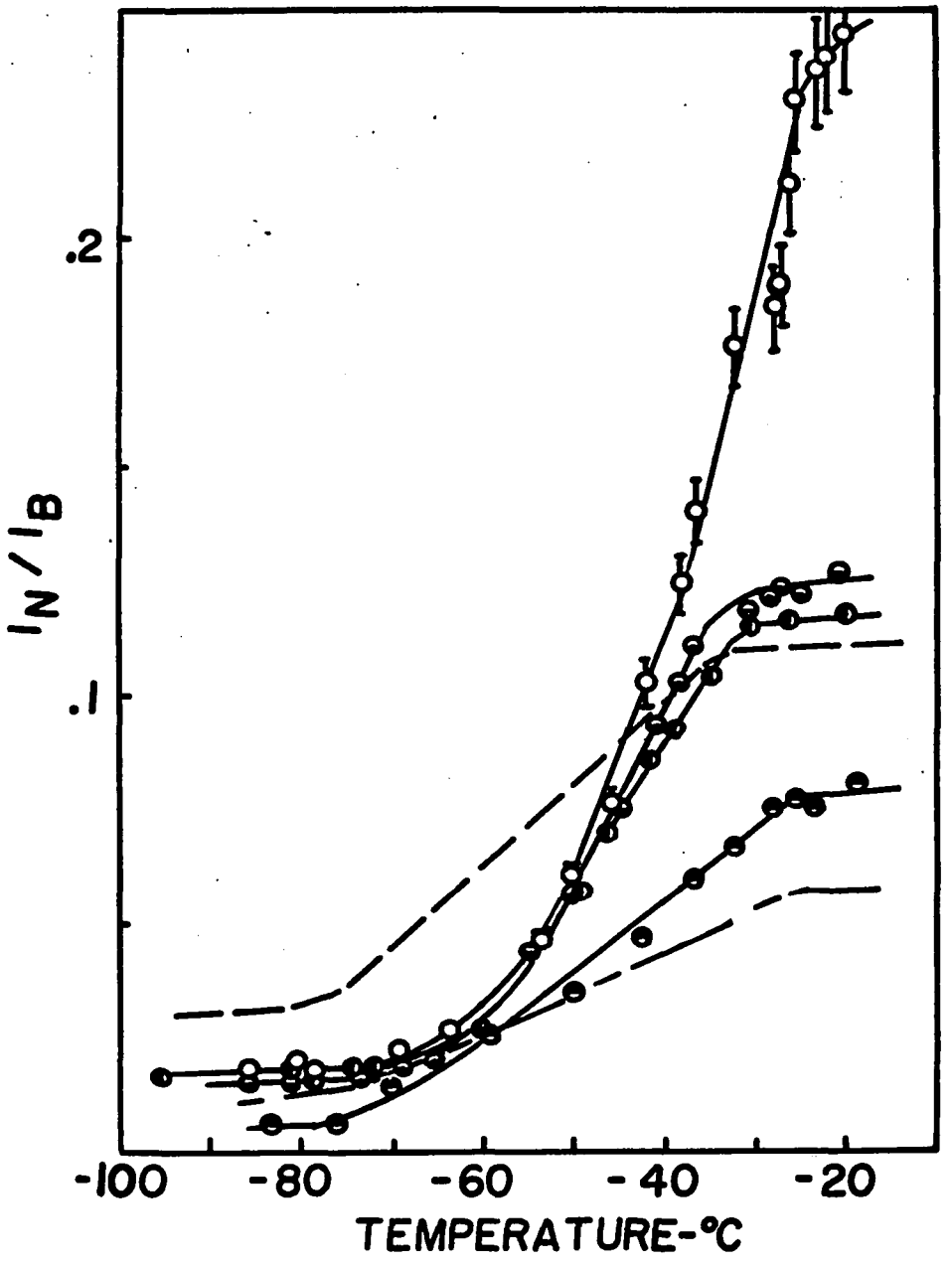

Figure 22. NMR narrow line-broad line intensity ratio vs. temperature for CS_2 wetted, 150°C annealed P4MP1(I)(A) crystals (●), 150°C annealed P4MP1(I)(T) crystals (●), 200°C annealed P4MP1(I)(A) crystals (●), 230°C annealed P4MP1(I)(A) crystals (O), as grown P4MP1(I)(A) crystals (---), and as grown P4MP1(I)(T) crystals (-·-).

ature region (above -35°C in this case) in which I_N/I_B is constant. At temperatures above -35°C, the I_N/I_B values are in the ratios: 1.0 : 1.1 : 2.0 for CS_2 wetted P4MP1(I) crystals grown from toluene, xylene, and amyl acetate respectively.

The N.M.R. intensity ratio of P4MP1(I)(A) crystals decreases two-fold faster than that of P4MP1(I)(X) and P4MP1(I)(T) crystals with decreasing temperature (see Fig. 21).

At -80°C, I_N/I_B of CS_2 wetted toluene grown crystals is 0.012; I_N/I_B of CS_2 wetted xylene grown crystals is 0.018 and I_N/I_B of CS_2 wetted amyl acetate grown crystals is about 0.03, which is 2.5-fold larger than that for Toluene grown crystals. I_N/I_B of CS_2 wetted xylene grown crystals is constant in the temperatures below -69°C.

The intensity ratio of CS_2 wetted P4MP1(II) crystals grown from amyl acetate is about 1.1 times larger than that of the toluene grown crystals in the temperature region above -35°C (see Fig. 21). For both preparations, the plot of I_N/I_B vs. temperature in the -35°C to -70°C region have the same slope, 0.9, which is ½ times that found for P4MP1(I)(A) crystals. In the temperature region below -70°C, I_N/I_B for these two samples become constant with the amyl acetate grown crystals having I_N/I_B value greater by a factor of 1.7.

In the temperature region above -35°C, the I_N/I_B of the CS_2 wetted P4MP1(I)(A) crystals (multilayered) is 0.011 which is about two-fold larger than that of the CS_2 wetted

P4MP1(II)(A) crystals (single layered). Similar results were found earlier for polyethylene by Blundell and co-workers;[34] in that study multilayered crystals of polyethylene were shown to have larger N.M.R. mobile fractions than single layered crystals of the same polymer.

It is seen from Fig. 22 that after heat treatment of dried P4MP1(I)(T) crystals at 150°C for 24 hours, I_N/I_B of the CS_2 wetted sample is 1.4 times larger than that of the original crystals wetted with CS_2 in the temperature region above -35°C. The slope of the I_N/I_B vs. temperature plot in the -35° to -63°C region is three fold larger for the annealed crystals than for the originals. In the temperature region below -70°C, I_N/I_B is constant at 0.006.

I_N/I_B in the temperature region above -35°C for the 150°C, 200°C, and 230°C annealed, CS_2 wetted P4MP1(I)(A) crystals increases by 5%, 12%, and 120% respectively, compared to that for the CS_2 wetted original crystals. In addition, I_N/I_B for these three samples decreases 1.7, 2.2, and 4.2 times faster with temperature from -35° to -55°C respectively than that for the original crystals. I_N/I_B becomes constant in the temperature region below -70°C, where it has values of 0.12 for both 150°C and 230°C annealed crystals, and 0.09 for 200°C annealed crystals. The results from Fig. 21 and Fig. 22 are listed in Table VI.

Fig. 23 shows plots of N.M.R. I_N/I_B versus time after CS_2 is added to dried P4MP1 crystals at -50°C. The same type of plot for heat treated P4MP1(I)(T) crystals and P4MP1(I)(A) crystals at -50°C are given in Fig. 24.

Table VI. The N.M.R. Crystallinities of P4MP1 Crystals.

Crystal preparation	Thermal history	I_N/I_B vs. temp. curve slope (btn.-55°to-35°C)	I_N/I_B (above -35°C)	Crystal-linity
P4MP1(I)(A) 135°C/100°C	as grown	1.70	0.11	0.90
P4MP1(I)(A) 135°C/100°C	150°C 24 hrs.	2.89	0.12	0.89
P4MP1(I)(A) 135°C/100°C	200°C 2 hrs.	3.74	0.13	0.88
P4MP1(I)(A) 135°C/100°C	230°C 2 hrs.	7.14	0.24	0.81
P4MP1(I)(T) 90°C/58°C	as grown	0.88	0.056	0.95
P4MP1(I)(T) 90°C/58°C	150°C 24 hrs.	1.48	0.078	0.93
P4MP1(I)(X) 90°C/60°C	as grown	1.10	0.06	0.94
P4MP1(II)(A) 135°C/100°C	as grown	0.88	0.058	0.94
P4MP1(II)(T) 90°C/58°C	as grown	0.90	0.052	0.95

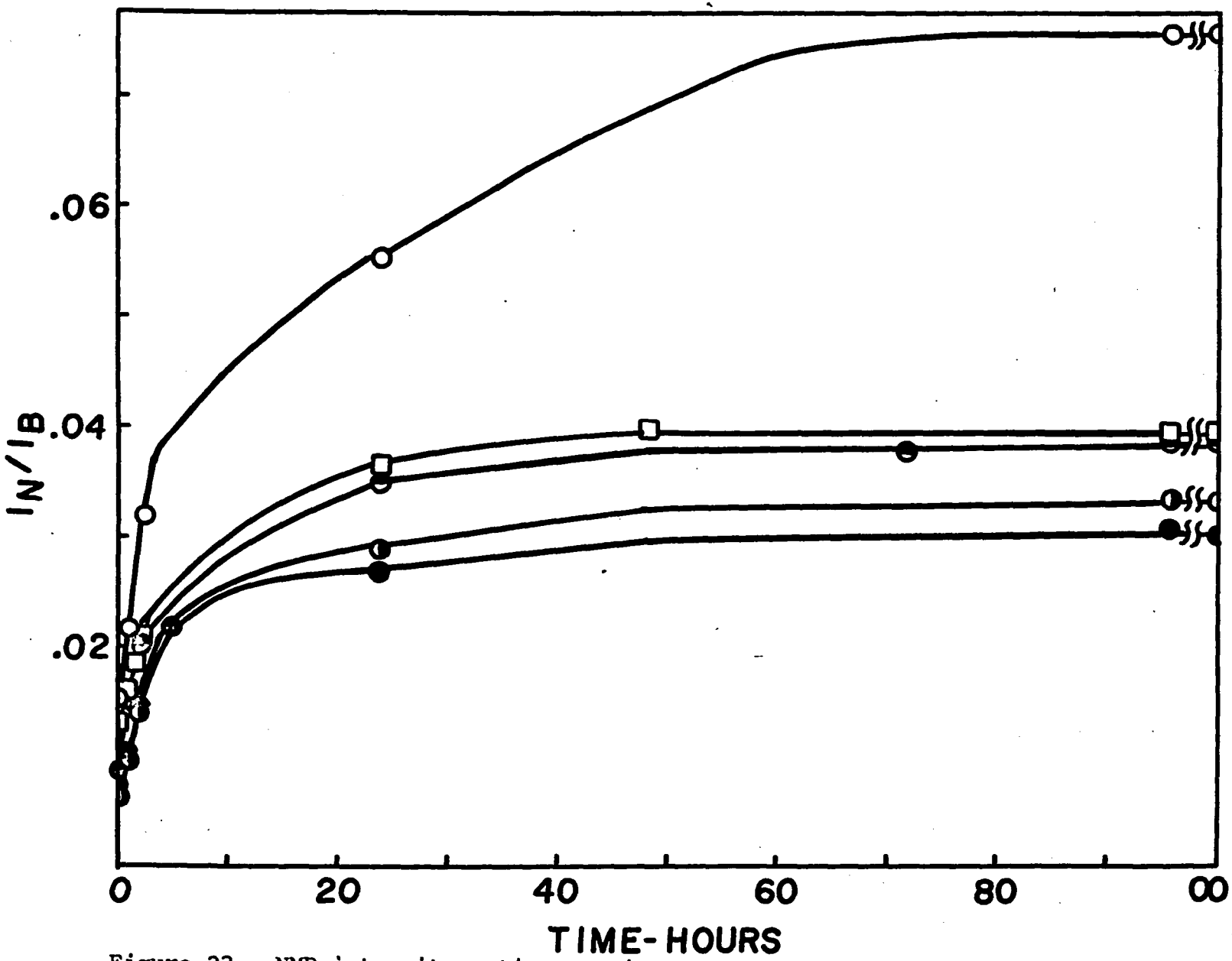

Figure 23. NMR intensity ratio vs. time after CS_2 is added to the dry, as grown P4MP1(I)(A) crystals (O), P4MP1(I)(T) crystals (O), P4MP1(I)(X) crystals (⊖), P4MP1(II)(A) crystals (□), P4MP1(II)(T) crystals (●).

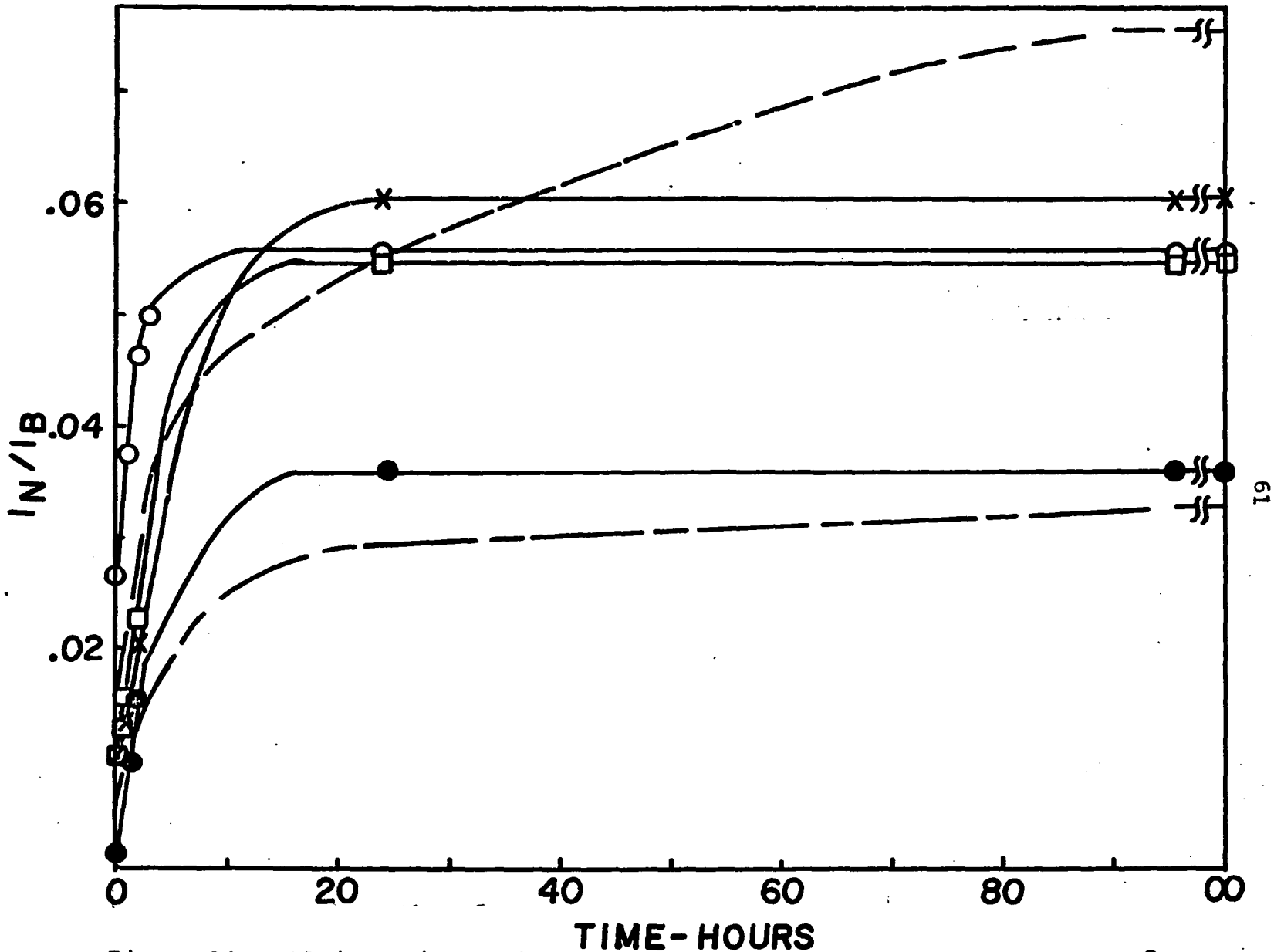

Figure 24. NMR intensity ratio vs. time after CS_2 is added to the dry 150°C annealed P4MP1(I)(A) crystals (□), 200°C annealed P4MP1(I)(A) crystals (O), 230°C annealed P4MP1(I)(A) crystals (X), 150°C annealed P4MP1(I)(T) crystals (●), as grown P4MP1(I)(A) crystals (---), and as grown P4MP1(I)(T) crystals (-——-).

I_N/I_B of all preparations of the crystals as grown needs more than 24 hours to become constant, while I_N/I_B of the heat treated crystals ceases to increase before 24 hours of time after CS_2 is added.

The rate of the I_N/I_B increase, within the initial three hours after CS_2 is added, of the crystals as grown is in the following order: P4MP1(I)(A)>P4MP1(I)(X)>P4MP1(I)(T)= P4MP1(II)(T)=P4MP1(II)(A) (see Table VII for values).

For the toluene crystals, the rate increases about two-fold after annealing at 150°C for 24 hours. The behavior of the P4MP1(I)(A) crystals is different. The rate first increases by 17% for the crystals annealed at 150°C for 24 hours, and then increases by 1½ fold for the 200°C annealed crystals. After 230°C annealing, the rate decreases to about that found for the as grown sample.

RESULTS ON EXPERIMENTAL ERROR ESTIMATION

The precision in the N.M.R. intensity ratio measurement in this study was found to be ±5%, as estimated in the manner described in the experimental section.

In comparing the N.M.R. results of the two different preparations of P4MP1(I)(A) crystals, it was found that the second preparation has slightly smaller I_N/I_B values in the temperature region between -35° to -15°C, and also has lower N.M.R. intensity ratio values in -63° to -35°C region, but the differences are within 5%. At temperatures below -63°C, I_N/I_B of the second preparation decreases slowly and shows a tendency to become constant. At -83°C, the

Table VII. The Initial Rates of I_N/I_B Increase after CS_2 Is Added to the Dry P4MP1 Crystals.

Crystal	Thermal history	Rate of I_N/I_B increases (initial 3 hours)
P4MP1(I)(A)	as grown	0.006/hour
P4MP1(I)(A)	150°C annealed	0.007/hour
P4MP1(I)(A)	200°C annealed	0.009/hour
P4MP1(I)(A)	230°C annealed	0.006/hour
P4MP1(I)(T)	as grown	0.004/hour
P4MP1(I)(T)	150°C annealed	0.007/hour
P4MP1(I)(X)	as grown	0.005/hour
P4MP1(II)(A)	as grown	0.004/hour
P4MP1(II)(T)	as grown	0.004/hour

same intensity ratio is found for both preparations of P4MP1(I)(A) crystals.

DISCUSSION

CRYSTAL PREPARATION

The PTBD single crystals and the P4MP1 single crystals prepared from amyl acetate and xylene using the self-seeding technique are uniform in crystal size. This is consistent with the fact that all the crystals start to grow simultaneously from nuclei already present. Since the crystal size is uniform, each individual crystal is representative of the preparation as a whole. P4MP1 crystals with two different sizes were obtained when toluene is used as the crystallization solvent. This indicates that the nuclei, from which the crystals are grown, form at two different times, with the larger crystals being formed from the nuclei first present.

Unlike the method which was employed to grow P4MP1 single crystals by Frank, Keller, and O'Connor,[84] who found the appearance of the P4MP1 single crystal not to be reproducible but to depend in an unpredictable manner on the cooling rate, the P4MP1 single crystals grown using the self-seeding method are reproducible.

Stellman[88] found that there is no difference in crystal thickness for PTBD single crystals grown from n-heptane dilute solution at 68°C and at 63°C. This may indicate that the thickness of PTBD single crystals are independent of the crystallization temperature. Rybnikar and Geil[51] have grown large regular tetragonal P4MP1 crystals at various temperatures in the range of 25 to 85°C from 0.01% xylene solution.

The thickness of these crystals was found to be 100 ± 10 Å, independent of the crystallization temperature. During preliminary work associated with the study presented herein, it was found by examining amyl acetate grown P4MP1 crystals using the electron microscope, that if the temperature is abruptly lowered during the crystallization, a small step appears on the surface of the lamellae, increase in temperature during crystallization results in a reverse step in the crystal, the new growth being thicker than the previous crystallized material. These findings are contrary to the experimental results of Tybnikar and Geil.

A reason for obtaining single crystals with thickness independent of temperature was given earlier by Jackson and Mandelkern.[52] From data relating the crystallization time of polyethylene to the time required to attain thermal equilibrium, they concluded that the relatively small change of the crystal thickness is a consequence of nonisothermal crystallization, the crystallization process being completed at higher temperature before the selected temperature is attained. Therefore, it is not meaningful to draw any conclusion about the temperature dependency of the single crystal thickness without further data relating the crystallization time to the time required for the polymer solution to attain thermal equilibrium.

The thickness of the P4MP1 crystal lamellae, grown in this study, were found to be independent of the melt flow index of the polymer. It was found previously by Keller

and O'Connor[55] that the lamellar thickness of polyethylene from fractions with average molecular weights between approximately 1000 and over 100,000, when crystallized at the same temperature, is the same. In the case of poly(ethylene oxide),[54] the long spacing is independent of the molecular weight for the polymers with molecular weight above 1500, providing the crystals are prepared at the same temperature from a given solvent. Sharma and Mandelkern,[57] and others[52, 89] concluded that for polyethylene single crystals, the internal and interfacial structure depends only on the crystal thickness, and is independent of the crystallization solvent. The present broad-line N.M.R. results indicate that this conclusion is not applicable to PTBD or P4MP1. The internal and interfacial structure found by this method is markedly dependent on the crystallization solvents at constant or near constant crystal thickness. Preliminary work also showed that there is no change in crystal thickness for either PTBD or P4MP1 crystals on storing for a long period of time at a constant growth temperature in any of the solvents used. This result indicates that the thickness of the polymer crystals is independent of the growth time at constant temperature. For P4MP1 single crystals grown from amyl acetate, the electron microscope result indicates that the crystal appearance is dependent on the polymer used. It is possible that this difference is due to a different rate of crystallization at the same temperature. The broad line N.M.R.

results indicated that this difference in appearance leads to different structure as will be discussed in the latter section.

THE STRUCTURE OF PTBD SINGLE CRYSTALS

The N.M.R. crystallinity as obtained from the narrow line to broad line intensity ratio in the -10^{o} to $-60^{o}C$ region for CS_2 wetted PTBD single crystals grown from dilute n-heptane and toluene solutions is given in Table V. The crystalline content for toluene grown crystals found by the present N.M.R. technique is significantly larger than that from I.R. (.5)[49] or DSC ($.6 \pm .1$). Therefore it appears that some amorphous parts of these crystals are not activated by CS_2. The higher crystalline content of the heptane-grown crystals is believed to be a consequence of growth at a temperature which is very close to the crystal-crystal transition temperature, whereas the toluene grown crystals are precipitated well below this transition temperature. At the temperature at which the n-heptane crystals were prepared, a considerable large-scale torsional motion is present in the polymer chains in the crystalline lattice. As cooling down to room temperature takes place, the polymer chains in the interior of the crystal have the opportunity to become ordered. When the toluene-grown crystals are prepared, the polymer chains cannot fit into the lattice slowly and therefore a higher amorphous content results.

The intensity of the viscoelastic loss peak at $-10^{o}C$

(110cps) is larger for benzene-grown PTBD crystals than the intensity of this peak for methyl-iso-butyl ketone grown PTBD crystals. Takayanagi et. al.[76] suggested that this difference in viscoeleastic behavior is due to a solvent effect. PTBD crystals with tighter folded loops are formed in the poorer solvent, MIBK.

Differential scanning calorimetry and infrared intensity measurements also suggest that toluene-grown PTBD crystals have a greater amorphous content than heptane-grown crystals (see Table II).

Upon comparison of the N.M.R. results with those from surface epoxidation studies (see Table II and V) some interesting facts emerge. The amorphous content relative to the crystalline content for the T crystals as seen by the N.M.R. technique exceeds the amount of material available at the crystal surfaces for epoxidation. Therefore, at least part of the amorphous regions available to CS_2 penetration are not available to the epoxidizing agent-metachloroperbenzoic acid, m-ClØCOOOH. This suggests that at least part of the amorphous material is below the crystal surface (interior amorphous regions). The amorphous component of the n-heptane grown crystals is located mainly on the crystal surfaces.

More direct N.M.R. evidence for the existence of these interior amorphous regions is the behavior of the N.M.R. narrow line with time upon addition of CS_2 to the dry material at a low temperature. It is expected that solvation of the disordered region at the surface would take place immediately while solvation of amorphous regions below the surface layer would take place at a slower rate. I_N/I_B would increase sud-

denly at the beginning, then show a period of more gradual increase, then finally level off, if the nonprotonated liquid is added at a temperature well below that at which the narrow line appears for the dried material. This effect is found for the toluene grown crystals but not for heptane grown crystals. It is seen that both the intensity ratio and the narrow line width are affected. This leads to a conclusion that a smaller amount, if any, of interior amorphous material is to be found in the heptane grown crystals than in toluene grown crystals.

It has been concluded from a number of previous investigations that the amorphous regions are on the crystal surfaces, either associated with the chain fold looseness[28,30] or with the presence of chain ends.[68] The DSC and I.R. results for toluene grown crystals suggest that this layer can involve half of the lamella and that only part of this is available for reaction with certain reagents such as mClØCOOOH.

The experimental results discussed above suggest that the three phase model[95-97] (Fig. 25) which includes a strained amorphous region (density gradient phase) could also be the model for polymer crystals grown from dilute solutions. In the strained amorphous region, the density is decreasing from the crystalline region density to the surface amorphous region density. This model was originally suggested for bulk polyethylene by Hoffmann and Lauritzen.[95] In the light of this model, it could be concluded that only the surface amorphous phase is available for reaction with mClØCOOOH, both the

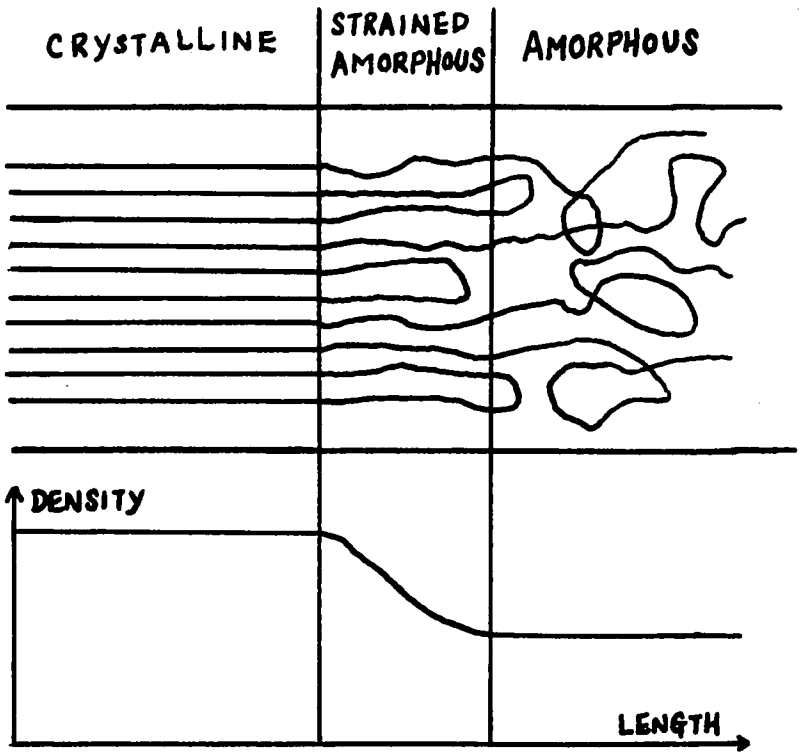

Figure 25. Three-phase model for polyethylene.[95-97]

surface amorphous and part of the strained amorphous phase (interior amorphous region) are available for CS_2 to penetrate; the solvation of the surface amorphous phase is almost immediate, while CS_2 penetrates into the strained amorphous phase at a relatively slower rate.

When the temperature of a polymer solution is decreased, the solvent power of the medium is reduced, if the chemical potential of the polymer species in solution exceeds the chemical potential which that polymer species would have in some solid phase; when this occurs the precipitation of that polymeric species takes place. The Gibbs free energy of the solute polymer contains not only a contribution from nearest neighbor interactions of solvent molecules with polymer segments but also a contribution resulting from the increase of configurational entropy accompanying the separation of the flexible chains from each other. However, both contributions should be proportional to chain length, and the solubility of polymer in poor solvents should fall off with their molecular weight[106] in a manner indicated by:

$$X_2 = e^{-AM_2} \qquad (6)$$

where A is a characteristic constant and M_2 is the molecular weight of the polymer solute. This equation indicates that polymer molecules with a higher molecular weight have lower solubilities and will precipitate from solution at relatively higher temperatures than polymer molecules with shorter chain lengths. A similar phenomenon is expected for polymer chains on the crystal surface when solvated by CS_2.

The longer unstressed polymer chain segments on the crystal surface will precipitate from CS_2 at a higher temperature than shorter stressed chain segments. Unstressed chain segments will precipitate from CS_2 at higher temperatures than stressed chain segments because the number of configurations available to unstressed chain segments are greater than that for stressed chain segments. Highly stressed amorphous segments may not be precipitated even at a temperature close to the freezing temperature of CS_2. Therefore, a gradual change in solubility means a distribution of different unstressed chain lengths and different degree of stress on amorphous chain segments.

At $-90^{o}C$, the N.M.R. narrow line component for the heptane-grown crystals has disappeared, while the intensity ratio is .13 for toluene grown crystals. This suggest that the amorphous segments which contribute to the narrow line absorption in heptane grown PTBD crystals are relatively unstressed as compared to the amorphous segments in the toluene grown crystals; about half of the amorphous segment existing in toluene grown crystals are under stress.

The slower decrease in intensity ratio for toluene grown crystals as compared with that for heptane grown ones with decreasing temperature below $-60^{o}C$ further suggests that there is a wider distribution of the degree of restraints on the amorphous segments for the toluene grown crystals.

Further information about PTBD crystals as grown has been obtained from crystal dissolution experiments. When as grown crystals suspended in toluene are resuspended in CS_2, the crystals dissolve within a few minutes at 25°C. Heptane grown crystals given the same treatment are only slowly attacked. After 60 days exposure, a number of crystals appear to have sustained little if any change. The difference in rate of dissolution could possibly be affected by a two fold difference in crystal size between toluene and heptane grown crystals. However, this can not account for the almost instantaneous solution of the toluene grown crystals by CS_2; it appears that this is evidence for a mosaic structure for these crystals. That is, there are disordered regions which traverse the crystal from one face to another, or from a face deep into the crystal interior.

Upon annealing the dried crystals of these two preparations at 80°C for five hours, a crystal thickening process occurs. This also leads to an increase in crystalline content for both samples as measured using the N.M.R. technique (see Table V). The difference in the N.M.R. intensity ratios for the two preparations disappears. Annealing PTBD crystals at higher temperatures (above 120°C) would bring about a decrease in crystallinity[76] as indicated by the reappearance of the mechanical loss peak at -10°C (110cps).[76]

At 80°C PTBD is in the high temperature crystalline form. X-ray results[78] show that the chains in the Form II lattice have a considerable amount of freedom and therefore

extensive rearrangements are possible. The differences in the heptane grown and toluene grown lamellae are therefore lost upon such treatment. Tatsumi et. al.[76] attributed changes in dynamic mechanical properties upon annealing from 60° to 110°C to chain fold tightening. However, the present results for the toluene grown crystals suggest that chain segments other than those in the fold can also be involved in rearrangements brought about by an annealing treatment. The observed increase in crystal thickness accompanying the annealing treatment would lead to a decrease in the number of folds but would not necessarily lead to fold tightening. Upon addition of CS_2 to dried samples of annealed toluene and heptane grown crystals, a narrow line immediately appears which does not show a change in intensity with time. This suggests that the amorphous component can now be found at the crystal surface only and that the interior amorphous regions have been reordered upon heat treatment.

THE STRUCTURE OF P4MP1 SINGLE CRYSTALS

Table VI shows the value of the crystallinity of P4MP1 crystals as obtained from N.M.R. intensity ratios. Upon comparision with the crystallinity of .66 obtained from the X-ray method,[47] it is concluded that complete penetration of the amorphous part by CS_2 is not taking place. It is seen that P4MP1(I) and P4MP(II), obtained from amyl acetate under the same crystallization conditions have different crystalline content, while those crystals of these two different polymers grown from toluene have the same crystalline content. It is clear that this behavior is due to differences in crystal morphology,

since the IA crystals are multilayered while those from the other four preparations are monolayered. This is contrary to the conclusion that crystallization processes are independent of solvent medium as suggested by Fischer and Hinrichen[98] and Blackadder and Roberts.[99] The crystalline fraction is found to depend on the preparation with an increase in the order: amyl acetate grown crystals < xylene grown crystals < toluene grown crystals for P4MP1(I). Sharma et. al.[57] also found that the density, as well as the crystalline fraction, of polyethylene crystals depends on the crystalline lamellae thickness. In the present study, the thickness is the same within experimental error.

From the I_N/I_B versus temperature plot for CS_2 wetted P4MP1 crystals grown from different solvents, it is found that at about -30°C an immobilization of the chain segments in the amorphous parts of the P4MP1 lamellae commences. The amount of the immobilization increases as the temperature decreases. However not all the chain segments become immobilized; about 0.5 to 1% are still actively reorienting in the low temperature region (-70°C). For the same reason as given for PTBD crystals, this spread in precipitation temperature is due to the varying degrees of restraint in the amorphous segments of the crystals.

The change in I_N/I_B versus time at -50°C for amyl acetate grown P4MP1(I) crystals wetted with CS_2 suggests that these crystals have a large amount of interior amorphous segments

which extend deep into the crystalline phase, so that, a longer time is needed for complete solvation.

Valuable information about the structure of P4MP1 crystals has been obtained from crystal dissolution experiments. When as grown crystals suspended in amyl acetate are resuspended in CS_2, the crystals dissolved within one minute at 25°C. Toluene grown crystals given the same treatment, as examined using the electron microscope, are torn apart into smaller pieces in a few minutes and then slowly attacked. These small parts of toluene crystals are about 1/20 of the original crystal size. After 20 days, these parts of toluene grown crystals appear to have sustained little if any change. This difference in rate of dissolution could not be affected by the difference in original crystal size between amyl acetate grown and toluene grown crystals, because amyl acetate grown crystals are the same size as the toluene grown large crystals and about two times larger than the toluene grown small crystals. It appears that this is evidence for a mosaic structure existing in both amyl acetate grown and toluene grown crystals with the crystal blocks being surrounded by amorphous regions. These results further suggest that these blocks are smaller for amyl acetate grown crystals than for toluene grown crystals.

Annealing of the toluene grown crystals at 150°C and of the P4MP1(I)(A) crystals in the 150°C to 230°C range leads to an increase in the amount of amorphous material available to CS_2 penetration (see Fig. 22). The increase in slope for the

I_N/I_B versus temperature plot in the -40° to -60°C region and the lowering of the intensity ratio for the annealed IA and IT crystals at the lowest temperatures used is consistent with relief of restraints on more highly strained amorphous segments. This stress relief would make the amorphous regions more uniform and thereby narrow the temperature range for precipitation of the amorphous segments from the CS_2 "solution" as well as leading to precipitation of a greater total number.

Annealing brings about a decrease in the time it takes for the CS_2 to penetrate all of the available amorphous regions (see Fig. 23 and Fig. 24), which suggests a greater uniformity of the amorphous regions after annealing.

Takayanagi and Kawasaki[47] have attempted to draw conclusions about the morphology of P4MP1 crystals from studies of the mechanical relaxation process at -150° to -160°C (110cps) and it seems appropriate to discuss their work at this time. In a dynamic mechanical relaxation study on P4MP1, Wall et. al.[107] attributed this low temperature process to motion of the isobutyl side chains. The dynamic mechanical loss peak manifested by this motion shows a tendency to split into two peaks and changes in crystal morphology lead to changes in the relative strengths of these two peaks. This behavior was interpreted by Takayanagi et. al.[47] in terms of a crystal model, in which small crystal blocks with slightly different orientation are assembled

Figure 26a. Schematic representation of the side view of the mosaic block structure of one lamella as given by Takayanagi and Kawasaki.[47]

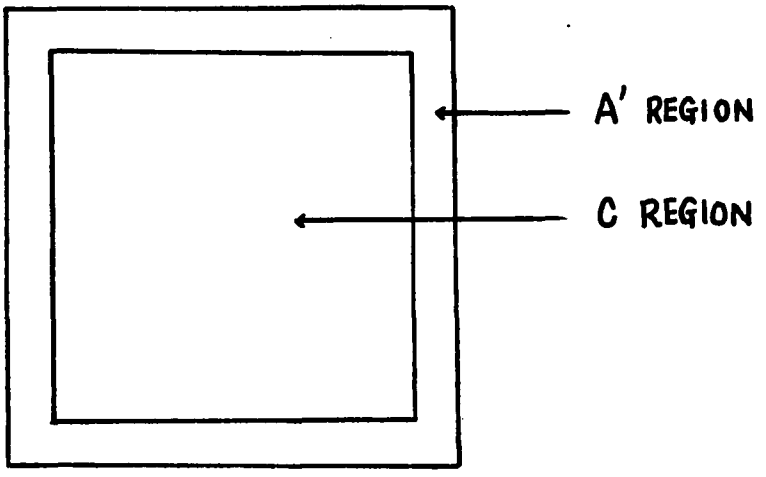

Figure 26b. A schematic mosaic block of P4MP1 (end surface of lamella).

(see Fig. 26). The lateral zones of these mosaic blocks are supposedly crystal defect regions, A', and are assumed to be part of the crystal region in calculation of the crystallinity. In addition to the mosaic blocks there are surface amorphous regions, A, associated with the loose chain folds and chain ends on the crystal surface. Therefore, the crystal region with perfect regularity, C, is surrounded by defect regions and surface amorphous material. An increase in both the A and A' region and a decrease in the C region are reported upon annealing xylene grown crystals at 195°C for three hours. The present work suggests that the A' regions between the crystal blocks can be penetrated by CS_2. Therefore some or all of the defect regions appear as amorphous material in the present N.M.R. investigation. These strained amorphous segments may not be solely located in the zones between the mosaic blocks, but may also be located in a region near the surface.

THE AMORPHOUS COMPONENT IN POLYMER CRYSTALS

Chain folding in polymer single crystals is an accepted phenomenon,[8] but the precise structure of the folds or the nature of the amorphous regions is still an active area of research.

Three different types of folds have been proposed for polymer single crystals: the irregular adjacent re-entry fold,[21] the regular adjacent re-entry fold,[24,25] and the switchboard or nonadjacent re-entry fold.[28,26] It has recently been concluded,[40,41] based on an infrared study on

polyethylene crystals consisting of a mixture of normal and deuterated hydrocarbons, that there is adjacent chain re-entry. Another feature on the surfaces of polymer single crystals is the presence of non-re-entry chain ends, or cilia.[90] Chemical assay on PTBD single [74] crystals also leads to the conclusion that polymer chain ends are on the crystal surface.

Michael and Bixler[91] concluded, from their gas solubility results, that a polymer crystal is a simple two phase system comprised of crystalline and amorphous regions, and the amorphous portion is considered to be analogous to a hydrocarbon liquid. A crystal lamella model is given by Takayanagi et. al.[76] for PTBD crystals grown from benzene solution. It is also a two-phase structure which includes a loose loopy chain folded amorphous layer and a crystal core (see Fig. 2). The same model was used for elucidation of experimental results by Peterlin and Meinel,[31] Fischer and Schmidt,[28] Flory,[30] and Keller and Priest.[68] A recent model of the crystal lamella suggested by Keller et. al.[35] is illustrated in Fig. 27a,b,c,d. This model postulates reentrant folds which are buried (27a), which are at the surface and bulging (27b,c) and which are at the surface and tight (27b,c) as well as loose hairs or cilia (27d) and non-reentrant folds (27d).

Based on the discussion in the above sections, it is obvious that a strict two-phase model in which the amorphous regions are associated with chain fold looseness and cilia is incorrect for PTBD and P4MP1 crystals. The crystal model must include interior strained amorphous material. In

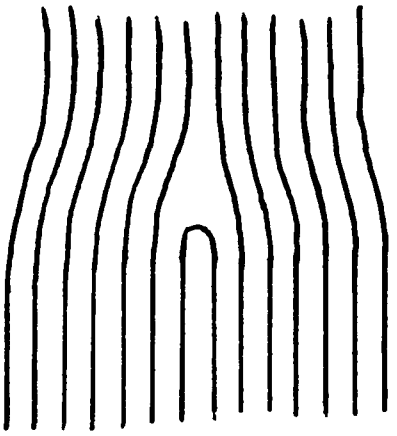

Figure 27a. Crystal defect due to a single fold buried deep inside the crystal.

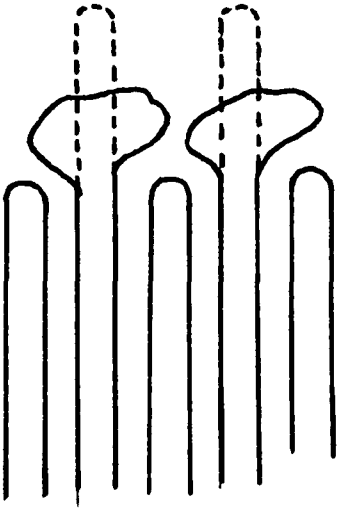

Figure 27b. Bulging out of folds due to several folds terminating at a lower level around them. The dotted lines show the straightened form of the bulging folds.

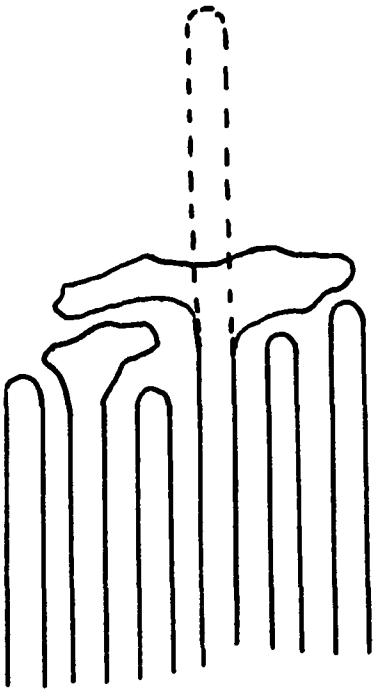

Figure 27c. Attempt to illustrate how a single, isolated fold protrusion would spread out in a disordered fashion onto its surrounding fold environment.[35]

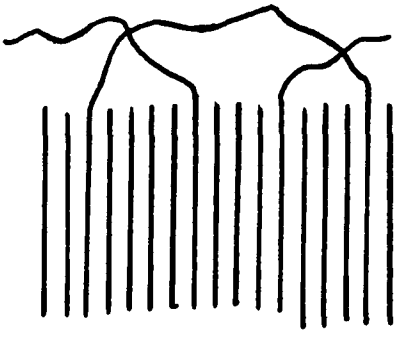

Figure 27d. A nonadjacently reentrant loose fold and examples of a short and long 'hair' overlying the rest of the fold surface, which is to be visualized as consisting of adjacently reentrant folds as in Fig. 27a,b,c but not drawn out here.

fact, for some crystal preparations the latter may exceed the amount of the amorphous material associated only with the surface portions of the chain fold and the loose chain ends.

The mosaic block model was first presented by Hosemann et. al.[92,93] to interpret the distortion of the crystal lattice. The mosaic structure of a polymer crystal is believed to form in the process of crystallization. This structure was suggested by the mode of plastic deformation found for P4MP1 single crystals.[94] It was also applied by Takayanagi and Kawaski[47] to elucidate the mechanical relaxation results for P4MP1 single crystals as discussed above.

It is believed that the three phase model[95-97] could be the correct model representing polymer single crystal structure.

SUMMARY

A broad line N.M.R. investigation at low temperatures on PTBD and P4MP1 single crystals grown from various solvents and subsequently wetted with carbon disulfide has been carried out. These data combined with previous chemical assay, infrared, and thermodynamical studies on PTBD single crystals suggest that interior amorphous regions, in which the amorphous segments are under stress, are located in polymer single crystals grown from dilute solution. The physical nature of these amorphous regions is found to be affected by the conditions of crystal preparation, such as the crystal growth temperature and the solvent used, as well as the crystal morphology, and the crystal thermal history.

The structure of polymer single crystals grown from dilute solution can be represented by a three phase model which has a strained amorphous phase as previously suggested for bulk polyethylene.

A distribution of stress on the amorphous segments is also suggested by considering the temperature dependence of I_N/I_B for CS_2 swollen crystals in the as prepared and annealed states. A different distribution of stress is found for crystals from different preparations. Relief of the strain on the highly stressed amorphous segments in polymer single crystals is manifested by the increase in slope of the N.M.R. narrow line to broad line intensity ratio versus temperature plot as well as the drop in this ratio at the lowest temperature of this plot for annealed P4MP1 crystals.

Crystal dissolution experiments suggest a mosaic block structure for dilute solution grown PTBD and P4MP1 single crystals.

REFERENCES

1. O. Schweitzer, Zeit. Z. Kr., 70, 206 (1919).
2. H. Standinger, R. Singer, Z. Z. Krist., 70, 139 (1929).
3. E. Sauter, Z. Phys. Chem., B18, 417 (1932).
4. H. Standinger, M. Standinger, E. Sauter, ibid, B37, 403 (1937).
5. E.W. Fischer, Z. Naturforsch., 12a, 753 (1957).
6. A. Keller, Phil. Mag., (8)2, 1171 (1957).
7. P.H. Till, Jr., J. Polym. Sci., 24, 301 (1957).
8. P.H. Geil, "Polymer Single Crystals", Interscience, New York (1963).
9. D.J. Blundell, A. Keller, J. Macromol. Sci-Phys. B2, 301 (1968).
10. P.H. Geil, N.K.J. Symons, R.G. Scott, J. Appl. Phys., 30, 1516 (1959).
11. D.A. Blackadder, J. Macromol. Sci-Revs. Macromol. Chem., C1, 297 (1967).
12. P.H. Geil, J. Polymer Sci., 44, 449 (1960).
13. E.W. Fischer, Z. Naturforsh., 14a, 584 (1959).
14. A. Peterlin, J. Appl. Phys., 31, 1934 (1960).
15. A. Peterlin, E.W. Fischer, Z. Physik, 159, 272 (1960).
16. A. Peterlin, E.W. Fischer, Chr. Reinhold, J. Chem. Phys., 37, 1403 (1962).
17. T.P. Lin, Unpublished calculations.
18. F.P. Price, J. Chem. Phys., 31, 1679 (1959).
19. F.P. Price, J. Polym. Sci., 42, 49 (1960).
20. J.I. Lauritzen, Jr., J.D. Hoffman, J. Chem. Phys., 31,

1680 (1959).

21. A. Keller, Kolloid Z., 197, 98 (1964).
22. V.P. Holland, P.H. Lindenmeyer, J. Appl. Phys., 36, 3049, (1965).
23. J.D. Hoffman, Soc. Plastic Eng., 4, 315 (1964).
24. P.H. Geil, J. Polym. Sci., 47, 65 (1960).
25. J.D. Hoffman, J.I. Lauritzen, E. Passaglia, G.S. Ross, L.J. Frolen, J.J. Weeks, Kolloid-Z., 231, 564 (1969).
26. J.P. Flory, J. Am. Chem. Soc., 84, 2857 (1962).
27. E.W. Ficsher, R. Lorenz, Kolloid-Z., 189, 97 (1963).
28. E.W. Ficsher, G. Schmidt, Angew. Chem., 74, 551 (1962).
29. J.B. Jackson, P.J. Flory, R. Chiang, Trans. Faraday Soc., 59, 1906 (1963).
30. P.J. Flory, J. Am. Chem. Soc., 84, 2857 (1962).
31. T. Kawai, A. Keller, Phil. Mag., 8, 1203 (1963).
32. A. Peterlin, G. Meinel, J. Polym. Sci., B3, 1059 (1965).
33. A. Peterlin, G. Meinel, H.G. Olf, J. Polym. Sci., B4, 399, (1966).
34. D.J. Blundell, A. Keller, T. Connor, J. Polym. Sci., A2, 5, 991 (1967).
35. A. Keller, E. Martuscelli, D.J. Priest, Y. Udagawa, J. Polym. Sci., A2, 10, 1807 (1971).
36. A. Keller, Y. Udagawa, J. Polym. Sci., A2, 1793 (1971).
37. R.G. Brown, J. Appl. Phys., 34, 2382 (1963).
38. J.C. Koenig, D.E. Witenhafer, Macromol. Chem., 99, 193, (1966).

39. J.C. Koenig, M.J. Hannon, J. Macromol. Sci-Phys., B1, 119,(1967).

40. S. Krimm, M.I. Bank, Preprints of Papers Presented at International Symposium on Macromolecular Chemistry, Toronto, Canada, A6, 18 (1968).

41. M.I. Bank, S. Krimm, J. Appl. Phys., 39, 4951 (1968).

42. T. Kawai, T. Goto, H. Maeda, Kolloid-Z., 223, 117 (1968).

43. T. Okada, L. Mandelkern, J. Polym. Sci., B4, 1043 (1966).

44. Y. Udagawa, A. Keller, J. Polym. Sci., A2, 9, 437 (1971).

45. H. Schonhorn, J.P. Luongo, Macromolecules, 2, 366 (1969).

46. J.B. Nichols, J. Appl. Phys., 25, 840 (1954).

47, M. Takayanagi, N. Kawasaki, J. Macromol. Sci-Phys., B1, 4, 741 (1967).

48. H. Hendus, G. Schnell, Kunststoffe, 51, 69 (1961).

49. C. Hendrix, D.A. Whiting, A.E. Woodward, Macromol., 4, 571,(1971).

50. N. Neto, C. diLauro, Eur.,Polym. J., 3, 645 (1967).

51. F. Rybnikar, P.H. Geil, J. Macromol. Sci-Phys., B7(1), 1 (1973).

52. F. Jackson,, L. Mandelkern, Macromolecules, 1, 547 (1968).

53. S-B Ng, J,M. Stellman, A.E. Woodward, J. Macromol. Sci-Phys., B7(3), 539 (1973).

54. F.J. Balta Calleja, A. Keller, J. Polym. Sci., A2, 2171, (1964).

55. A. Keller, A. O'Connor, Polymer, 1 (1960).

56. D.W. McCall, W,P. Slichter, J. Am. Chem. Soc., 80, 1861, (1958).

57. R.K. Sharma, L. Mandelkern, Macromol., 3, 578 (1970).

58. W.P. Slichter, J. Appl. Phys., 31, 1865 (1960).

59. D.J. Blundell, A. Keller, I.M. Ward, I.J. Grant, J. Polym., Sci., B4, 781 (1966).

60. D.W. Slichter, D.W. McCall, J. Polym. Sci., 230 (1957).

61. R.C. Rempel, H.W. Weaver, co-workers, J. Appl. Phys., 28, 1082 (1957).

62. H. Thurn, Kolloid-Z., 179, 11 (1960).

63. R.L. Collins, Bull. Am. Phys. Soc., Ser. II, 1, 216 (1956), Ser. II, 2, 139 (1957).

64. D.W. McCall, E.W. Anderson, J. polym. Sci., A1, 1175 (1963).

65. S. Iwayanagi, I. Sakurai, J. Polym. Sci., C14, 29, (1966).

66. A.E. Woodward, A. Odajima, J.A. Sauer, J. Phys. Chem., 65, 1384 (1961).

67. T. Williams, D.J. Blundell, A. Keller, I.M. Ward, J. Polym. Sci., A2, 6, 1613 (1968).

68. A. Keller, D.J. Priest, J. Macromol. Sci., B2, 479 (1968).

69. A. Keller, D.J. Priest, J. Polym. Sci., B8, 13 (1970).

70. V.K. Bermann, K. Nawotki, Kolloid Z. Z. Polym., 219, 132 (1967).

71. V.K. Bermann, K. Nawotki, Kolloid Z. Z. Polym., 250, 1094, (1972).

72. S. Iwayanagi, I. Miura, Rept. Prog. Polym. Phys. Japan, 8, 303 (1965).

73. J.M. Stellman, A.E. Woodward, J. Polym. Sci., B7, 755 (1969).

74. J.M. Stellman, A.E. Woodward, J. Polym. Sci., A2, 9, 59 (1971).

75. B.A. Newman, J.M. Stellman, A.E. Woodward, J. Polym. Sci., Polym. Phys. Ed., 10, 2310 (1972).

76. T. Tatsumi, T. Fukushima, K. Imada, M. Takayanagi, J. Macromol. Sci-Phys., B1, 459 (1967).

77. S. Takamuku, T, Tasumi, M. Takayanagi, Reports on Progress in Polymer Science in Japan, X, 333 (1967).

78. S. Iwayanagi, I. Sakurai, T. Sakurai, T. Seto, J. Macromol. Sci-Phys., B2, 163 (1968).

79. M. Takayanagi, N. Kawasaki, J. Macromol. Sci-Phys., B1, 4, 741 (1967).

80. G. Natta, P. Corradini, Porri, Rend. Acad. Nazl. Lincei, 20, 728 (1956).

81. G. Moragio, G. Polizzotti, F. Danusso, Eur. Polym. J., 1, 183 (1965).

82. K. Suehiro, M. Takayanagi, J. Macromol. Sci., B4, 39 (1970).

83. J.M. Stellman, A.E. Woodward, S.D. Stellman, Macromolecules, 6, 330 (1973).

84. F.C. Frank, A. Keller , A. O'Connor, Phil. Mag., 4, 8, 200, (1959).

85. M. Litt, J. Polym. Sci., A1, 2219, (1963).

86. J.H. Griffith, B.G. Ranly, J. Polym. Sci., 44, 369, (1960).

87. D.R. Morrow, G.C. Richardson, L. Kleinman, A.E. Woodward, J. Polym. Sci., A2, 5, 493 (1967).

88. J.M. Stellman, Ph.D. Thesis, The City University of New York (1972).

89. T.W. Husby, H.E. Bair, J. Appli. Phys., 39, 4969 (1968).

90. S. Krimm, M.I. Bank, J. Polym. Sci., A2, 7, 1785 (1969).

91. A. Michael, H. Bixler, J. Polym. Sci., 50, 393 (1961).

92. R. Hosemann, J. Appli. Phys., 34, 25 (1963).

93. R. Hosemann, W. Wilke, F.J.B. Calleja, Acta Cryst., 21, 118 (1966).

94. A.E. Woodward, D.R. Morrow, J. Polym. Sci., A2, 7, 1651 (1969).

95. J.D. Hoffmann, J.I. Lauritzen, J. Res. Nat. B. Stand. 65A, 297 (1961).

96. H.G. Killian, H. Linz, F.H. Muller, H. Ringsdorf, Kolloid-Z. u. Z. Polymere, 202, 108 (1965).

97. V.K. Bergmann, K. Nawotki, Kolloid-Z. u. Z. Polymere, 219, 132 (1966).

98. E.W. Fischer, G. Hinrichen, Kolloid-Z. u. Z. Polymere, 219, 93 (1966).

99. D.A. Blackadder, T. Roberts, Macromol. Chem., 126, 116 (1969).

100. I.I. Rabi, J.R. Zacharias, S. Millman, P. Kusch, Phys. Rev., 53, 318 (1938).

101. C.P. Slichter, "Priciple of Magnetic Resonance", Harper & Row, Publishers, Inc., New York (1963).

102. A. Abragam, "The Principle of Nuclear Magnetism", Oxford University Press, Fair Lawn, N.J. (1961).

103. A. Carrinton, A.D. McLachlan, "Introduction to Magnetic Resonance with Application to Chemistry and Chemical Physics", Harper & Row Publishers, Inc., New York (1967).

104. C.W. Wilson, III, G.E. Pake, J. Chem. Phys., 27, 115 (1957).

105. R. Endo, Nippon Gomu Kyokaishi, 34, 527 (1961).

106. H. Morawetz, "Macromolecules in Solution", Interscience Publishers,(1965).

107. A.E. Woodward, J.A. Sauer, R.A. Wall, J. Polymer Sci., 50, 117 (1961).